uc3m | Universidad **Carlos III** de Madrid

Master Degree in Aeronautical Engineering
2020-2021

Master Thesis

Design of the AOCS system of a 6U satellite for Earth and Space observation

Rodrigo Santos García

Mario Merino Martínez
Antonio Flores Caballero
Madrid, first of July 2021

SUMMARY

Keywords: Attitude determination, guidance, pointing, system sizing, nanosatellite

DEDICATION

For those who may find this work useful for their own learning.

CONTENTS

LIST OF FIGURES

LIST OF TABLES

1. INTRODUCTION

The need of satellites to point towards a certain direction in a controlled manner is a problem that can be decomposed in two separated issues, the estimation of the attitude itself and its later control. This aspect, that could be thought to lead to a coupling problem between both parts of the pointing process, in practice is not such. Generally, all attitude determination and control systems fulfill its pointing requirements if, separately, the estimation and control requirements are fulfilled. As explained in [22], this is an idea that, theoretically, only applies to linear systems (Separation theorem), but that practically can usually be assured for non-linear systems as that of the dynamics of a satellite.Consequently, in order to to fulfill certain pointing requirements, both aspects could generally tackled separately. This differentiation is, in fact, one of the key features to distinguish the different eras regarding satellite pointing history.

The importance of pointing was raised since the first artificial satellite was launched, the Sputnik, on 1957, as it is commented in [3]. This field is a more than 60-year area whose development is discussed on the introduction of [22]. Three main stages can be differentiated considering the estimation-control duality and the evolution of computation and power/cost capacity:

- The first twenty years, that are mainly explained in [3], in which several estimation algorithms were developed such the *algebraic method point-by-point* by Black in 1964 [23] or the *q method* by Davenport [3] in 1978, amongst others. However, these algorithms were computationally too costly for the on board computer capacity at this time so they were executed on ground and punctual retroalimentation of the system was performed , as explained in [22]. Consequently, space mission at that time had to be provided with passive attitude control systems (gravity gradient, spin stabilization) that were able to maintain certain attitude without continuously knowing its own attitude.

- The second era started with the QUEST algorithm development [24] and on board application for the HEAO 1-3 missions. From this moment on, with the increasing computation capacity of the missions, and the advanced development of Extended Kalman Filters, missions started to increase its pointing requirements. This increase has its paradigm in the demanding pointing levels of the Hubble Space Telescope (Launched in 1990). After several on-orbit astronaut work, the telescope was able to point for certain sustained periods of time, with an accuracy of 0.007 arc sec [25].

- This second era of the space missions tending to be bigger, more powerful and, generally, maximizing pointing requirements can be considered to be finished in the moment the nanosatellites have started to rise their number of launches per year. As can be observed in Figure 1.1, since 2013, when the number of launches

raised from 25 to 88, this number has never fallen bellow this level. In fact, more than 750 nanosatellites are forecast to be launched by 2025. This trend, although probably not being yet so important in budget terms, is expected to lead the market in number of launches in the following decades.

This new paradigm of space commercialization, shifting from public monopoly to private aperture, frequently known as New Space [27], has a direct impact in pointing requirements. Now, a compromise between acceptable accuracy (0.1 to 1°) and volume/ mass and power budget has to be reached. This comes from the the restrictions in terms of space and mass that standard nanosatellites must comply with, as it is stated in [4] for a 6U satellite, as it is the case for this work: launch mass lower than 12 kg and total volume within an envelope of 100 X 226,3 X 336 mm.
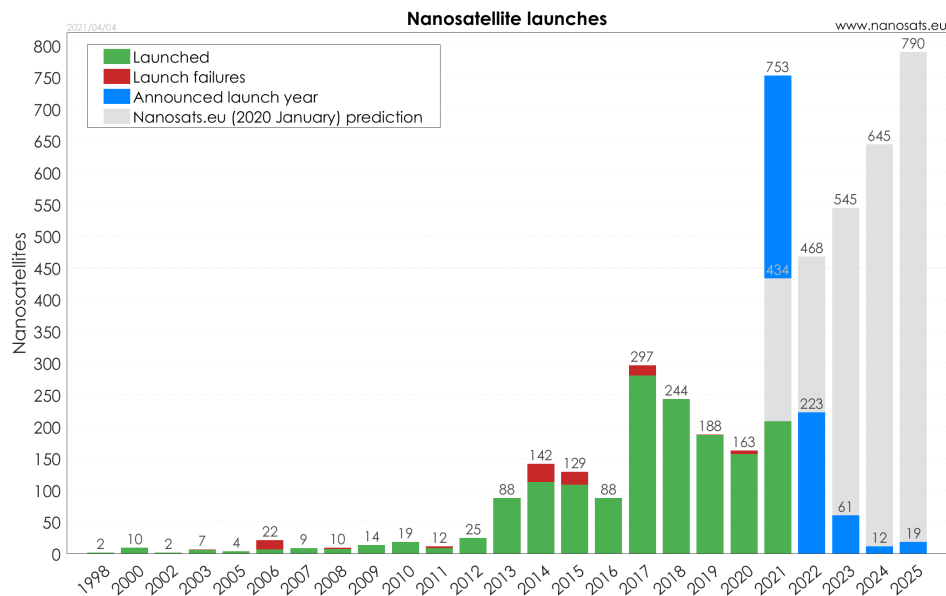
Fig. 1.1. Number of nanosatellites (Volume from 0.25U to 27U) launched from 1998 and forecast up to 2025 [26]

Direct consequence of the development of New Space is the MartinLara Mission (ML) [28]. This project intends to develop a 6U nanosatellite platform for airborne validation of low TRL technologies with certain attitude control needs, regarding Nadir/Zenith pointing specially. Such pointing requirements are stated in the Mission Requirement Document (MRD) [29]. Consequently, this project intends to provide the development of the Attitude and Orbit Control System for the ML mission, fulfilling the requirements stated in [29]. It must be noted that, such development, would require more than one final master thesis to be fully accomplished and tested. Thus, this document focuses on the evaluation of the feasibility of the most restricting attitude requirements from a theoretical and practical software implementation approach.

An important remark is that, although a thruster is intended to be embarked as payload,

its command will not be used as first approach for orbital corrections. Thus, the AOCS system will only be focused on the attitude determination and control of the satellite, and so this work accordingly.

2. STATE OF THE ART

Regarding the current state of the art of the AOCS design, there are several references to consider. Some of them are a bit old but still valid, such as Wertz's *Spacecraft attitude determination and control* [3]. Others are more educationally oriented such as Markley´s *Fundamentals of Spacecraft Attitude Determination and Control* [22]. These two, among other big references such as Fortescue et al. [1] or Pisacane [5] are traditional baseline for AOCS designing. However, due to the clarity and conciseness of table 19-1 depicted in [8], regarding the AOCS design process, it has been considered as the main reference to structure this section and the actual design of the system explained afterwards. An adaptation of this table is shown below and, as can be observed, the 6 steps explained there are the reference for this section structure.

Step	Inputs	Outputs
1a) Control modes definition 1b) System requirements derivation	Mission requirement document	Control modes Constraints
2) Disturbance environment quantification	Geometrical features and orbit definition	External torques values
3) Type of spacecraft control per mode	Payload thermal and power needs Orbit end environment Accuracy needed	Control method needed (single axis stabilization through gravity, spin..., or three-axis)
4) Select and size hardware	Accuracy needed Power available Mass and volume restriction	Set of sensor, actuators and data processing hardware
5) Define determination and control algorithms	Performance needed Power, thermal and mechanical limitatons	Exact software for attitude determination and control in each mode and logic transition between them
6) Iteration and documentation	All the previous	Detailed definition of the previous

Table 2.1. AOCS DEFINITION STEPS [8]

2.1. Requirements definition

The task of defining the requirements of a space mission is probably the most critical one and, sometimes, one of the most neglected ones. From mission and, consequently, system requirements, the rest of the system definition is developed. Thus, several allusions are made through all traditional references as, for example in the first chapter of [1] and [5]. Nevertheless, it is in [6] where more detailed analysis of the topology of requirements and good practises for their definition are explained, as it will be explained below. This section also includes the basic features that requirements should comply with from a software development standpoint, as per [31]. Although satellite mission requirements are not directly applied to the software developed in the project, they must feature exactly the same characteristics as those applicable to software development.

Thus, these main features applicable to the satellite requirements are summarized in the following:

1. Unitary, it defines just one aspect of the system.

2. Complete, no information left to designer´s interpretation.

3. Consistent, no contradiction by itself or with other requirements or system reference documents.

4. Traceable, its source and reason to exist is well documented.

5. Atomic, without compound written expressions.

6. Unambiguous, clear language without non-specific acronyms or abstract concepts is used.

7. Verifiable, the means of compliance and verification are well defined and are achievable within the scope of the project.

8. Current, the requirement is still valid at the present day of the project.

Once these features are assured for the mission requirements, several considerations must be taken for the system requirement definition, as per [6].

The main one is to consider what is to be done instead of how it is going to be accomplished, In that way, the trade off analysis that is associated to each requirement is not previously biased from a mission point of view. Furthermore, a measurable mean to test the compliance with the requirement must be provided in order the requirement to be useful in a system designer approach. Together with these two disquisitions, a rationale behind the requirement must be provided. Why a requirement does exist is usually as important as being well posed. The reason for this is to avoid extra constraints in the system and to be able to trace down the source of each requirement.

As final conclusion, for the requirement definition process,it can be considered an alive process all through the project. Both from a mission and system standpoint, requirements are susceptible to change and to adapt to project changes, scope adaptations or unexpected events. From the system designer point view, requirements must be seen as the opportunity to determine and size not only its own system but also the necessary interfaces with other systems in the mission in order to iterate until convergence to the final design is reached.

2.2. Control modes definition

The first stage of the AOCS design, after havig the mission requirements defined, is to determine the modes in which the satellite may be pointing. But the first question to answer is, what does the word "mode" refer to? This is generally a very ambiguous concept whose main purpose is essentially to avoid ambiguity.

Firstly, one should consider a mode not only in the sense of pointing requirements needed to be fulfilled, but also in a general platform sense. There is a possibility that, with the same attitude mode, the whole satellite may be operating differently depending on the mission requirements (different signal state, failure, payload, ground commands...). Secondly, as stated in [30], the satellite cannot be in an undefined state. This need of definition makes the mode to be constructed as a set of parameters to be defined, as it is in [30]:

1. Kinematic target, defined as a certain inertial satellite orientation (quaternion, q) and an angular velocity in body frame (ω).

2. Sensors configuration.

3. Actuator configuration.

4. Attitude estimator configuration.

5. Attitude predictor configuration (if needed and implemented, not in this case)

6. Controller configuration

7. Satellite configuration

8. Entry conditions

9. Exit conditions

For each mode in which the system may be operating, this 9 parameters must be perfectly defined to avoid malfunctioning leading to satellite failure and mission loss. These 9 parameters are defined by two main aspects:

- Mission requirements needed to be fulfilled

- AOCS requirements derived from the previous restrictions and from the exact solution taken (sensors, actuators, algorithms...)

2.3. Environmental torques

Environmental torques are the main source of pointing perturbation for satellites. Apart from that, internal disturbance torques are the other way in which the intended attitude of the satellite is disturbed. A quick and concise view of such perturbations is depicted in Table 9.1 of [1] and is replicated in Table 2.2. It can be considered that only the first 4 external torques are applicable to the mission, and none of the internal torques are (no mechanisms, nor liquid fuel, astronauts or flexible parts are present). If reaction wheels

are present, they would be a rotating part but they would be considered as a control torque rather than an external one.

External torques	Range of potential predominance
Aerodynamic	<500 km depending on solar activity
Magnetic	500-35000 km
Gravity gradient	500-35000 km
Solar radiation	>700 km depending on solar activity
Thrust Misalignment	All heights
Internal torques	
Mechanisms	
Fuel movement	
Astronaut movement	All heights
Flexible parts	
Other masses movement	

Table 2.2. POINTING PERTURBATION TORQUES

These torques are present in the AOCS design process in two steps. For the sizing of the actuators and sensors, question that will be addressed with more detail in section 3.3. And for its representation in the Dynamic and Kinematics Environment model [32], implemented to complement this work. This second part is the one needed to test the performance of the AOCS software before implementing it in a physical device during lab tests

2.4. Satellite stabilization topology

Depending on the attitude control necessities of a satellite mission, the way the system needs to control its pointing is different. The main categories are stated in section 3 of [1], and can be summarized as:

1. No momentum biased - 3 axis stabilized.

   In this case, active and continuous internal torque is provided to counteract disturbance torques. Usually requires more complex software and higher power needs.

2. Momentum biased.

   A continuous spinning part of the satellite provides the platform with an angular momentum that, through the gyroscopic effect, helps the spacecraft to maintain the intended attitude. Three different cases exist within this type of attitude stabilization:

   - Spinner.

The whole satellite rotates along one of its axis to control its attitude. Reduces hardware and software complexity but is not valid for most of the usual payloads (just one axis-pointing an always rotating).

- Dual-Spinner.

  Part of the satellite structure itself is used as rotating part to produce gyroscopic effect and gain attitude control capacity. Widens the number of possible payloads but increases heavily the platform mechanical integration.

- Hybrid

  Uses a continuous rotating device, momentum wheel, as attitude control device. This solution is easier in terms of integration as compared to the dual-spinner, but still has less attitude command capability than the 3-axis stabilised.

2.5. Attitude determination and control algorithms

Regarding the software to determine and control a satellite´s attitude, there are several references to be considered, specially [3], [22] and [44]. No big detail on the mathematics will be here develop, this will be carried out in the section where the model developed is explained. However, an overall review of the different existing solutions is carried out.

2.5.1. Attitude determination

As can be seen in table 2.3, there are two main ways of determining attitude, by direct calculation (geometrically, algebraically) which are really problem dependant and not computationally efficient, and state vector estimation, whose utility is beyond any doubt and will be the solution taken in this thesis.

Type		Method	Advantages	Disadvantages
Attitude determination		Geometric	Conceptually easy	Inverse trigonometric functions Angular ambiguities
		Algebraic	Robust and conceptually easy	Not statistically optimal Needs 2 vector observations
		Q method	Optimize n measurements	Requires vector measurement (not possible for gyroscopes)
State vector estimation	Batch	Least squares	Simpler than recursive Less sensitive to bad data	Slow convergence for big state vectors. Big data storage needed
	Recursive	Least squares	Less data storage Faster convergence	More sensitive to bad data Kalman filter captures state variations better
		Kalman Filter	Instantaneous attitude determination	Convergency problems Plant dynamics linearization
		Extended Kalman Filter	Captures non-linearities	Convergency problems
		Unscented Kalman Filter	Captures deeper non-linearities	Convergency problems Model complexity
		Sequential PseudoInverse	Useful with accurate observations and less accurate propagation process (Gyroscope and Star tracker combination) Computationally easier and faster than Kalman	General worse performance than Kalman

Table 2.3. ATTITUDE DETERMINATION ALGORITHMS BASED ON [3] AND [22]

2.5.2. Attitude control

Regarding attitude control software, although new approaches, such as neural nets or artificial intelligence, are being implemented, traditional linear proportional- derivative control will be applied.

2.6. MATLAB and Simulink implementation and testing

In order to develop the algorithms needed for attitude determination and control of the satellite, the use of MATLAB and its tool Simulink has been chosen. The first reason for this choice is to take advantage of its graphic interface for the reduction of implementing times. This coding format allows for quick program adaptations and trials that, with a linear coding program could take ten times or even more time to be implemented. The second advantage of using this language is its source code, C, that is standard thanks to its robustness, for real time operation systems as it is the case of a nanosatellite.

3. AOCS DESIGN AND JUSTIFICATION

3.1. Mission requirements

The following requirements are obtained from the Martin Lara mission requirement document, ML-0004-SYS-IDR, reference [29]. Only those mission requirements that could have any impact on the AOCS definition are written in this section.

3.1.1. Requirement definition

In order to define each requirement, the following format requirement, [R/G]-[MX]-[YYY]-[ZZZ], is used in [29] and is followed here:

- Requirement Severity (R/G):

  R, **mandatory**, requirements with shall construction.

  G, **desirable**, requirements with should construction.

- Requirement source (MX)

  In this case, M X indicates the objective, as defined in [29], that acts as source for each specific requirement.

- System applicability (YYY)

  This indicates the spacecraft system to which the requirement applies, being the possible acronyms the ones that follows:

    - MIS Mission Requirement
    - PYL Payload requirement
    - ORB Orbit analysis requirement
    - ADC Attitude determination and control subsystem requirement
    - EPS Electrical power Subsystem Requirement
    - STR Structure requirement
    - COM Communications subsystem requirement
    - DHS On-board Data-handling subsystem requirement
    - TCS Thermal control subsystem requirement
    - PRO Propulsion subsystem requirement
    - CNF Configuration requirement

- Requirement number (XXX)

  Correlative unique identification number

3.1.2. Mandatory

- R-M0-ADS-010: **Nadir pointing accuracy** by 3 x Nadir antennas shall be of **1 deg**.

- R-M0-ADS-020: Nadir attitude determination by 3 x Nadir antennas shall be known with an accuracy of 0.1 deg with respect to Nadir.

- R-M0-MIS-030: Absolute position of the spacecraft shall be determined with better accuracy than 10 m (Root Mean Square error).

- R-M0-MIS-040: Time stamping (UTC) at which any on board event has taken place shall be known with an accuracy better than 0.1 seconds.

- R-M2-PYL-120: The Sun penetration in the FOV of each Nadir antenna shall be recorded as a function of time.

- R-M2-PYL-170: Measurements with any radiometer pair shall be taken for a complete orbit as a minimum.

- R-M4-PYL-210: A FOV of 90 deg (± 1 deg) half angle along Zenith Radiometer´s normal shall be free of the Sun, Earth and spacecraft obstacles during operation.

- R-M4-PYL-220: The Sun and the Earth penetration in the FOV of each Zenith antenna shall be recorded as a function of time.

- R-M6-MIS-290: The spacecraft shall comply with the Cubesat design standards.

3.1.3. Desirable

- G-M0-ADS-015: Nadir pointing accuracy by 3 x Nadir antennas should be of 0.05 deg.

- G-M0-ADS-025: Nadir attitude determination by 3 x Nadir antennas shall be known with an accuracy of 0.05 deg with respect to Nadir.

3.2. AOCS modes identification

In order to satisfy the requirements previously stated, the AOCS system shall have a certain architecture. This architecture (lines of operation and modes) are shown in figure 3.1. This configuration is considered to be the minimum one to fulfill all the requirements minimising the complexity of the system and its validation. This explanation is qualitative so, in forthcoming sections, after analysing the performance needed, a more detailed specification on which actuators, sensors and software are used in each mode will be given.

SBM: Stand-By Mode
DtM: Detumbling Mode
DsM: Desaturation Mode
FPM: Fine Pointing Mode (Non-Inertial)
EM: Eclipse Mode
SM: Safe Mode

Operatonal Lines

FDIR: Fault Detection, Isolation and Recovery
NOM: Nominal operation
ECL: Eclipse transition
Nominal from launcher ·······
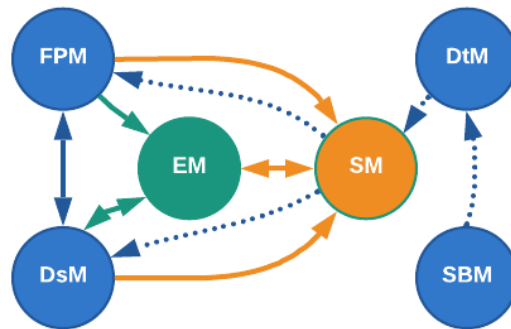
Fig. 3.1. AOCS modes scheme

The scheme shown before is described in the following:

- **Nominal Line**: This is the group of modes and transitions between them that will be occurring during operation without failure (in blue).

  - Stand-By Mode (SBM)

    The system is still attached to the launcher, so the on board computer is in stand by and ready to start working.

  - Detumbling Mode (DtM)

    This mode would start operating when the spacecraft detects an anomalously high angular velocity that would imply it is out of the launcher/deployer. The spacecraft shall be able to reduce its angular velocity to a certain value yet to be defined in which the rest of the modes of the nominal line are able to operate normally.

  - Fine Pointing Mode (FPM)

    In this mode, the spacecraft shall be able to point towards Nadir/Zenith with a minimum attitude accuracy of 1 deg, knowing its current accuracy with a minimum of 0.1 deg, as stated in section 3.1.

  - Desaturation Mode (DsM)

    Since the satellite is not using any thruster to carry out neither orbit or attitude control, the attitude control system needed shall be a reaction wheel or any other moment accumulation device. In the requirements it is also stated that the accuracy must be known with certain accuracy, in all three axis, which defines the satellite to be a 3-axis stabilised one. Consequently, a 3-reaction wheel system has been chosen as command components devices. Thus, there is a mode, this desaturation one, that shall assure that the reaction wheels

reduce their angular velocity to a certain, value yet to be defined, after having reached their saturation level.

- **Fault detection isolation and recovery line**: This is the line in which the satellite will enter in safe mode if a failure is found in any of the vital subsystems of the spacecraft.

  - Safe Mode (SM). This mode will make the satellite to remain pointing towards the Sun, in such a way that only the minimum number of subsystems are active, maximizing the amount of energy received and minimizing the possibility of new failures. The satellite would remain that way until communication occurs with the ground station, moment in which the telemetry data of the satellite would be received and could be analysed to determine if the satellite is able to recover the nominal line or not. This mode need a low gain antenna to communicate with the ground station without pointing directly towards it, and a robust attitude sensor (coarse sun sensor) to determine the attitude of the spacecraft. This mode will also be used as initial one after detumbling to charge batteries to the maximum level possible prior to the start of nominal operation.

- **Eclipse transition**: In the type of orbit chosen as baseline, a Dawn-Dusk Sun synchronous one of 500 Km, the number of eclipses is minimum. However, as there is a possibility of having them, this line would be in charge of managing such situation.

  - Eclipse Mode (EM). During this mode, the satellite shall be able to maintain the operability of the system after leaving the eclipse phase. This means that, depending on the final sizing on the batteries and the power need of the AOCS system and others during eclipse (thermal, payload...), there are two main possibilities:

    1. Leave the satellite to freely rotate and, when the eclipse finishes, recover normal operation through a detumbling of the angular momentum gained.
    2. Maintain the last attitude before eclipse (minimize attitude perturbations) during the eclipse duration. This one would only be possible if batteries are big enough and are charged above a certain level yet to be defined.

    It is also remarkable that the level of saturation of the reaction wheels will also be critical for this mode. If there is no margin for them to keep desaturating the system during the whole eclipse, a free-rotating eclipse mode may be needed whatever the

An alternative modes configuration was proposed as shown in Figure 3.2 in order to reduce the number of modes in one. The detumbling mode would disappear and the safe mode would be in charge of managing the angular speed resulting from satellite

deployment. However, it was assessed that the increase in difficulty when developing the attitude determination and control software would we greater than the ease gained due to the disappearance of one mode.
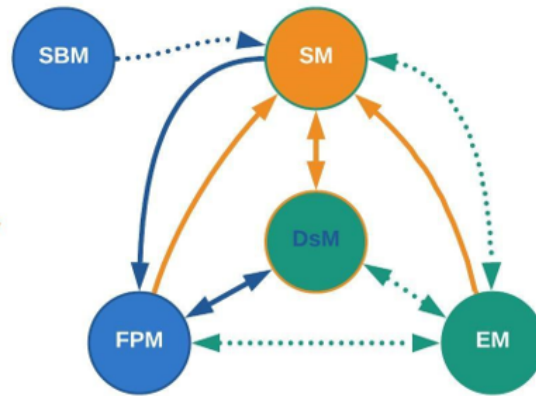
Fig. 3.2. Alternative AOCS modes scheme

3.3. Disturbance torque environment

In this section the disturbance environment within which the satellite will be operating is analyzed in order to size the actuators needed for its operation. Firstly, a dummy satellite has been considered, in a conservative way, such that the disturbance torques have a provision for this initial sizing. Then, using references such as [1],[3] or [6], a first estimation of the environmental torques have been calculated for the sizing of the momentum detumbling devices needed for the mission operation. Also, a more detailed calculation, solving for the momentum equations of the satellite, has been done, in order to refine the actuators needed.

In order to analyze the environmental torques that will be affecting the satellite during its operation, the orbit geometrical features and the relative position of the satellite within it has been analyzed in Figure 3.3. The angular considerations with respect to the Sun shown in this image are relevant parameters for solar panels and battery sizing (eclipse). Apart from that, what should be analyzed is the nominal position of the satellite. This, considering the body axes shown in Figure 3.4, is to have the Z axis parallel to Nadir-Zenith, the Y axis contained in the satellite orbit (tangent to its speed) and the X axis according to complete the right handed axes system.
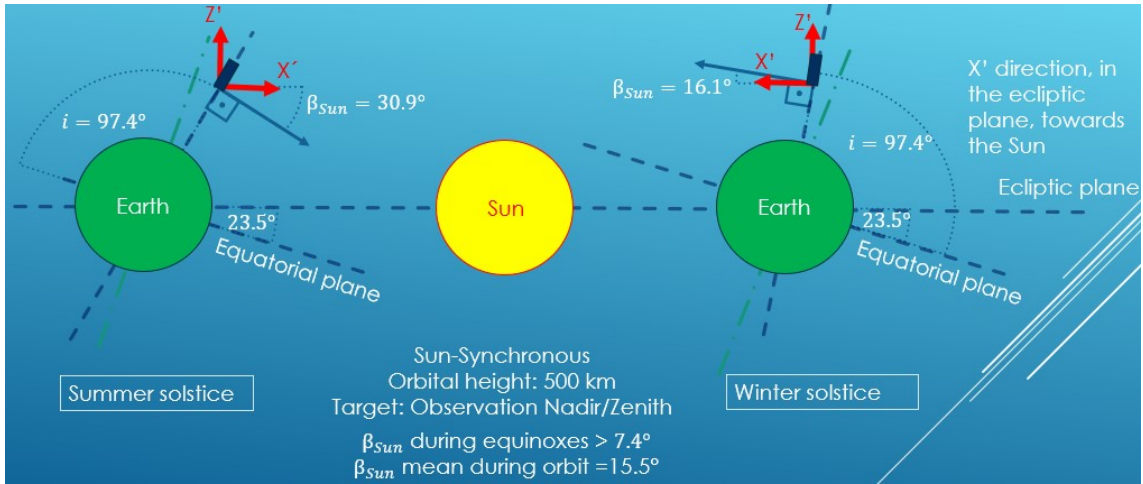
Fig. 3.3. MartinLara reference orbit with geometrical features during solstices and equinoxes

3.3.1. Dummy satellite definition for environmental torque determination

In order to determine the disturbances that will keep the satellite away from maintaining the desired attitude profile, an initial satellite shape and inertia has been proposed as shown in figure 3.4. This satellite is a $10 \times 20 \times 34,05cm$ cube (6 units, as the maximum proposed in the mission requirements of [9]). The mass considered has been the one for a typical cube sat, 1,33 kg/unit, resulting in 7,8 kg as total. The distribution, for the sake of conservatism, has been considered as 2 masses of 2,72 kg the orange ones in figure 3.4 and 1,36 kg for the green one, plus 1 kg for the outer structure.
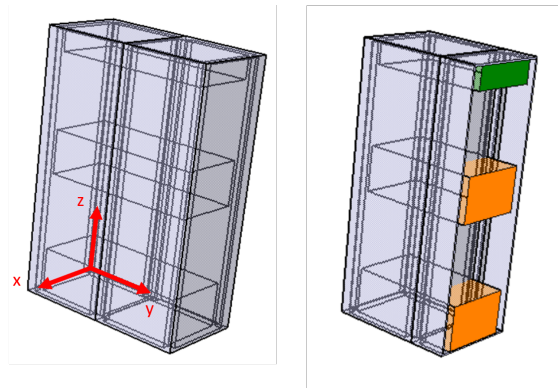
Fig. 3.4. Satellite dummy for environmental torque estimation

The resulting inertia properties are:

- Mass: 7.8 kg.

- Center of Gravity (CoG): Considering the body fixed axis system shown in figure 3.4, the CoG coordinates are:

    - $X_{CoG} = 0.05m$

- $Y_{CoG} = 0.1m$
- $Z_{CoG} = 0.1324m$

- $I_x = 0.083$ kgm^2

- $I_y = 0.101$ kgm^2

- $I_z = 0.027$ kgm^2

Apart from the inertia properties, the following features have been assumed for the calculation of the environmental torques:

- Effective drag area (m^2): 0,02

  This area corresponds to the face normal to the Y axis of Figure 3.4. This face will be the one perpendicular to the satellite speed during its nominal operation (Z axis Nadir pointing).

- Effective solar radiation pressure area (m^2): 0,1362

  This value accounts for a solar panel of double the maximum $0,0681m^2$ area face that will be generally facing the Sun. Its considered to be perfectly facing the Sun for the sake of conservatism, although, as shown in Figure 3.3, the mean angle of the panel with respect to the Sun will be 15.5°.

- Residual magnetic moment ($A \cdot m^2$): 0,2 normal to the Earth Magnetic field.

  As per Reference [33], the typical value of the residual magnetic moment goes from 0,1 to 20 $A \cdot m^2$. Considering that a 6U satellite is one of the smallest satellites to be launched, 0,2 is considered to be a reasonable assumption for the residual magnetic dipole. This assumption can be considered also as a target in further stages of the design for the residual magnetic dipole in the x body axis.

- Specular reflectivity factor f_{si}: 0.5

- Diffusive reflectivity factor f_{di}: 0.5

  These values implies that the external material of the satellite is in the middle point of being mirror-like $f_{si} = 1$, and being a perfect diffuser of the power reflected, $f_{di} = 1$.

- Drag coefficient, C_d: 2.5

  This value is typically in the range [2, 2.5], as per reference [6], so the conservative value has been taken.

3.3.2. Perturbation torques calculation

Regarding the direction of the perturbing torques, it is not known *a priori* and, probably, during the operation of the satellite, they could counteract each other. However, a worst case approach is again used and all will be summed as though they were applied in the same direction and with the same sign, as first approach.

1. **Gravity gradient torque**:

   Regarding the moment the satellite is subjected to due to the gravity gradient when describing a circular orbit, the following expression is considered from [6]:

   $$T_g = \frac{3\mu}{2R^3} \left| I_z - I_y \right| \sin(2\theta) \qquad (3.1)$$

   where T_g is the external torque due to gravity gradient, μ is the Earth's gravitational constant ($3.986 \times 10^{14}\ m^3/s^2$), R is the orbit radius (6871 km), I_z and I_y are the moments previously stated in kgm^2 and θ is the maximum deviation of the Z axis with respect to the local vertical, $\pi/4\,rad$ in this case, to maximize the moment.

   With all these data, the magnitude of the gravity gradient torque results $T_g = 1.36 \times 10^{-7} Nm$.

2. **Solar radiation pressure torque**:

   In order to estimate the solar radiation pressure torque, a solar panel of double the maximum area of the satellite facing perfectly the Sun has been considered. Thus, the following equations from [1] has been considered:

   $$\mathbf{T}_{\text{SRP}} = \sum_{i=1}^{n} \mathbf{r}_i \times \mathbf{F}_{\text{SRP},i}, \quad \mathbf{F}_{\text{SRP},i} = a_i \hat{\mathbf{s}} + b_i \hat{\mathbf{n}}_i \qquad (3.2)$$

   $$a_i = -PA_i \cos \theta_i \left(1 - f_{s,i}\right), \quad b_i = -2PA_i \cos \theta_i \left(f_{s,i} \cos \theta_i + \frac{1}{3} f_{d,i}\right) \qquad (3.3)$$

   where T_{SRP} is the torque, r_i is the distance between the panel center of gravity and the center of gravity of the satellite ($h_{sat}/2 - z_{CoG} = 0.03785m$), F_{SRP} is the force applied by the solar radiation pressure. P is the Earth mean momentum flux 4.67×10^{-6} N/m^2, A_i is the area of the plane considered, f_{si} and f_{di} are the specular and diffusive reflectivity coefficients and θ_i the incidence angle between the Sun and the panel, 0 rad in this case. Thus, considering the values stated before, the resulting torque is, $T_{SRP} = 3.21 \times 10^{-8} Nm$.

3. **Drag torque**:

For the drag torque calculation, the approach stated in [6] has been applied:

$$T\,aero = \frac{1}{2}\rho C_d A V^2 (C_{pa} - C_g) \qquad (3.4)$$

where ρ is the density at the height of the orbit, C_d is the drag coefficient, A is the effective drag area, V is the orbital velocity, C_{pa} is the pressure coefficient position and C_g is the center of gravity position.

In order to estimate the torque, a certain value of the density must be considered, obtained from the Figure 3.5, with an altitude of 500 km, a value of 10^{-12} kg/m^3 has been selected. The orbital velocity V is computed as Eq. 3.10 giving a value of 7.610 km/s.

$$V_a = \sqrt{\frac{\mu}{R}} \qquad (3.5)$$
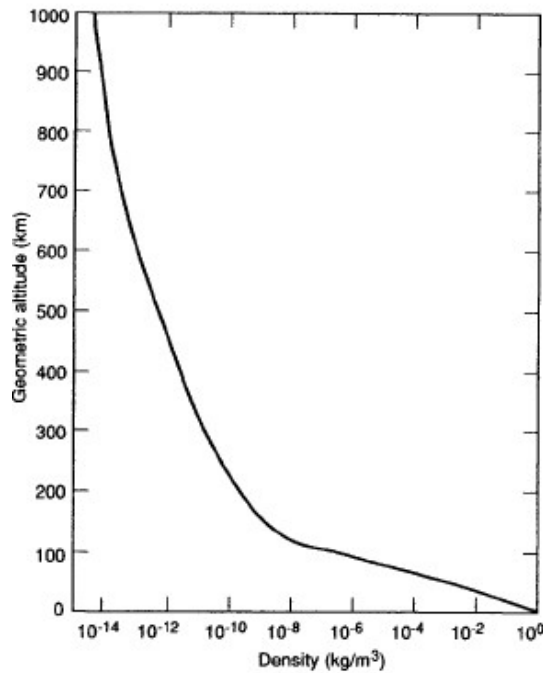
Fig. 3.5. Density over geometric altitude from reference [5]

Thus, considering a center of aerodynamic pressure placed at half the "effective chord" of the satellite face, 0,17 m from its base, and a safety factor of 10 due to the uncertainties of the aerodynamic behaviour of the satellite, the aerodynamic torque results $T_{aero} = \underline{5.48 \times 10^{-6} Nm}$

4. **Magnetic torque**:

As proposed in [1], the external magnetic moment **T**, is **T** = **m** × **B**, where, **m** is the residual magnetic moment of the satellite (represented as a dipole) and **B** is

the local magnetic flux density of the Earth. Considering an averaged value of the Earth magnetic field at 500 km of altitude bearing in mind figures 3.6 and 3.7, we get a magnetic flux density of 5×10^{-5} T, considering the maximum magnetic flux density at 90 of magnetic latitude (2 times that of the equator). With the value of the residual magnetic moment of the satellite previously stated, the resulting external torque due to the magnetic field of the Earth is $T_m = \underline{1.0 \times 10^{-5} Nm}$.
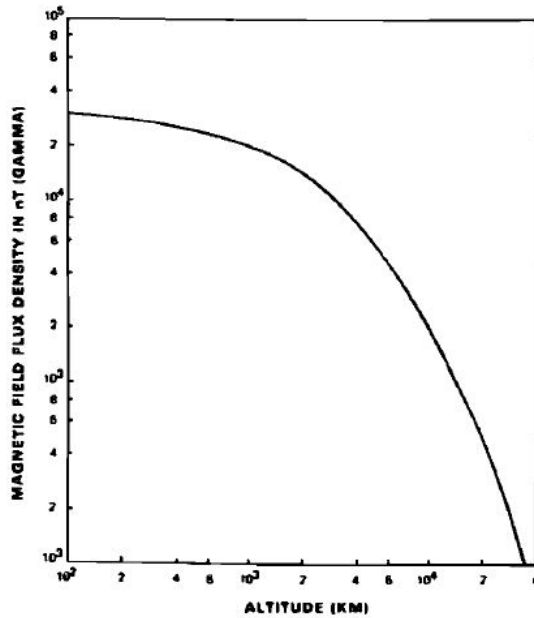
Fig. 3.6. Magnetic field flux over altitude from reference [3]
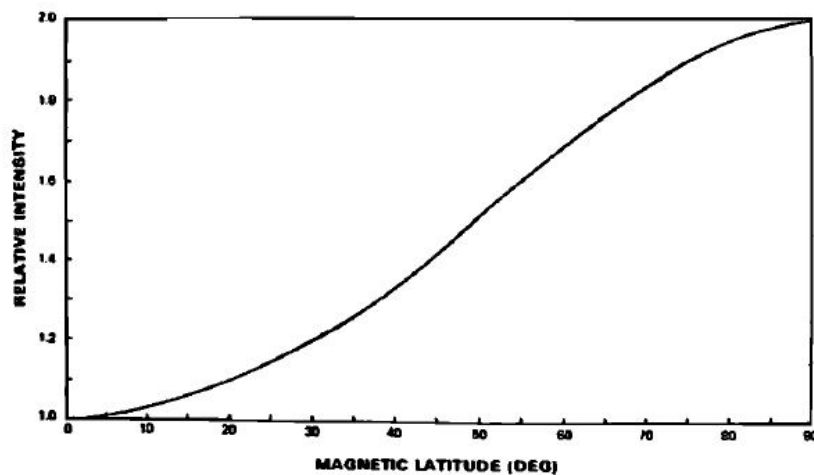
Fig. 3.7. Relative intensity of the magnetic field flux over magnetic latitude from reference [3]

Having considered all the possible environmental torques, it can be observed in Table 3.1, that the main contribution to attitude perturbation is the magnetic torque followed by the drag torque being both them 1 order of magnitude greater than the others. Consequently, after having chosen a set of actuators for desaturation with this first rough order

of magnitude of the perturbation torques, a refinement in this calculation will be done considering just the more relevant perturbation torques.

Torque	Max Value (mN·m)	Mean Value (mN·m)
Gravity gradient	1.36×10^{-4}	1.36×10^{-4}
Solar radiation presure	3.21×10^{-5}	3.21×10^{-5}
Drag	5.48×10^{-3}	5.48×10^{-3}
Magnetic	1.0×10^{-2}	7.50×10^{-3}
Total	0.0156	0.0131

Table 3.1. SUMMARY OF THE ENVIRONMENTAL TORQUES

3.4. Actuators and sensors

In general, two options for all the actuators and sensors are presented, one for fulfilling the mandatory requirements and other, more demanding, for the desirable ones. For the correct development of AOCS modes with the requirements needed, the following sensors and actuators have been chosen:

3.4.1. Actuators

Bearing in mind the level of accuracy needed, the actuators required for such good performance will be reaction wheels (Reference [6], page 173). For the desaturation of the wheels and for coarse manoeuvring, typically thrusters are used but, in this case, magnetorquers are chosen for the desaturation (Desaturation Mode), and reaction wheels will be used for attitude manoeuvres (Fine Pointing Mode).

Reaction wheels (RW)

For a 3-axis stabilised system as this satellite needs to be, three reaction wheels are the minimum needed to provide torque in three normal directions and a fourth one for redundancy could be used in case of failure.

In order to size the reaction wheels to be mounted, the following equations from [8] have been considered:

$$T_{RW} = \max\{T_{RW,d}, T_{RW,s}\} \tag{3.6}$$

$$T_{RW,d} = T_D(1 + SF) \tag{3.7}$$

$$T_{RW,s} = 4\theta \frac{I}{(t_s)^2} \tag{3.8}$$

$$H_{RW} = \frac{T_D \cdot P \sqrt{2}}{8} \tag{3.9}$$

where T_D is the average disturbance torque observed in Table 3.1. Regarding the slewing manoeuvres, the most critical one is considered to be the case in which the solar panels have to face perfectly the Sun in case of failure to enter the Safe Mode in the summer solstice. In that sense, I is the maximum moment of inertia of the satellite, $I_{yy} = 0,101 kgm^2$, $t_s = 1min$ is the minimum time required to perform a manoeuvre (typical value), $\theta = 30,9°$ is the maximum angle performed in a manoeuvre (see Figure 3.3 for Summer solstice manoeuvre), SF is the safety factor considered for the disturbance torque, 1,2 in this case and P is the orbital period of the satellite. Then, $T_{RW,d}$ and $T_{RW,s}$ are the resulting torque needed to compensate environmental disturbances and to carry out a slewing manoeuvre, respectively. Finally, T_{RW} and H_{RW} are the required torque and stored angular momentum required by the reaction wheels. T_{RW} needed is the one to perform the most critical slewing manoeuvre

Equation 3.9 considers that the perturbation has a sinusoidal shape (as the magnetic perturbation has, over the magnetic latitude variation), whose mean value is T_D. Since, as it has been considered in section before, the magnetic field is predominant in terms of torque disturbance, this assumption seems reasonable, taking into account that the mean disturbance torque would be $T_m = 1.58 \times 10^{-5} Nm$ considering a 20% margin.

Consequently, the minimum values needed, considering that all the torques need to be compensated by just one of the RW, are the ones shown in table 3.2.

$T_{RW,d}(mN \cdot m)$	0.0158
$T_{RW,s}(mN \cdot m)$	2.18
$T_{RW}(mN \cdot m)$	0.705
$H_{RW}(mN \cdot m \cdot s)$	15.8

Table 3.2. SIZING PARAMETERS FOR THE REACTION WHEELS

Magnetorquers (MT)

In the case of the magnetorquers, as it was for the reaction wheels, a minimum of 3 need to be installed, and 4 could be used for the sake of redundancy. It is true that no matter the attitude the satellite has, the magnetorquers will only be able to generate torque in two directions, perpendicular to the local magnetic field line. However, if having only three magnetorquers, a loss of one of them would imply the lack of capability of the satellite to desaturate a reaction wheel in one of the two perpendicular directions to the magnetic

field and, probably, the loss of pointing capability over the duration of the mission. This would be the reason to install 4 of them.

In order to size the magnetorquer needed, as explained in [8], the torque that the magnetorquer is able to produce must be equal to the disturbance environmental torque existing. Consequently, the magnetic moment the magnetorquer must be able to produce is:

$$D_{m,MT} = \frac{T_D}{m_{min}} \tag{3.10}$$

where $T_D = 0.016 mN \cdot m$ is the existing disturbance torque and $m_{min} = 2.5 \times 10^{-4} T$ is the minimum magnetic field over the orbit. Then, the minimum magnetic moment needed by the magnetorquer is $\underline{D_{m,MT} = 0.631 A \cdot m^2}$.

Nonetheless, it must be noted that this value is strongly dependant on the residual magnetic dipole of the satellite (the predominant disturbance torque is the magnetic one and is proportional to this dipole) and, consequently, this should be revised in more advanced stages of the design process. It must also be noted that the time the desaturation the satellite takes to be completed is also of concern and should be studied during the implementation phase of the desaturation mode.

Components off the shelf considered

With the purpose of meeting the requirements previously stated for both the reaction wheels and the magnetorquers, the following components are selected (2 options for each):

- Reaction Wheel RWP015 by Blue canyon Technologies

RWP015	
Momentum	0.015 Nms
Max Torque *	0.004 Nm
Mass	0.130 kg
Volume	42 x 42 x 19 mm
Voltage	12 VDC
Power @ 1/2 Momentum	< 0.6 W
Power @ Full Momentum	< 1.0 W
Design Life	> 5 years
Static Unbalance * (Fine)	< 1.2 g-mm (0.25 g-mm)
Dynamic Unbalance * (Fine)	< 20 g-mm² (2.5 g-mm²)

Fig. 3.8. First option of reaction wheels chosen [10]

- Reaction Wheel GSW600 by Gomspace

This option allows for an integrated pyramid configuration that would occupy a bit more than one half unit, in a compact and multi functional option.

One Wheel

Description	Value	Unit
Mass	180	g
Size	44.0 x44.0 x 27.0	mm
Flywheel inertia	300	gm²

Pyramid
Mounting bracket and 4 wheels.

Description	Value	Unit
Mass	940	g
Size	95.0 x 95.0 x 61.6	mm

2.1 **Highlighted Features**
- 3-year design lifetime
- 2 mNm torque
- 19 mNms storage
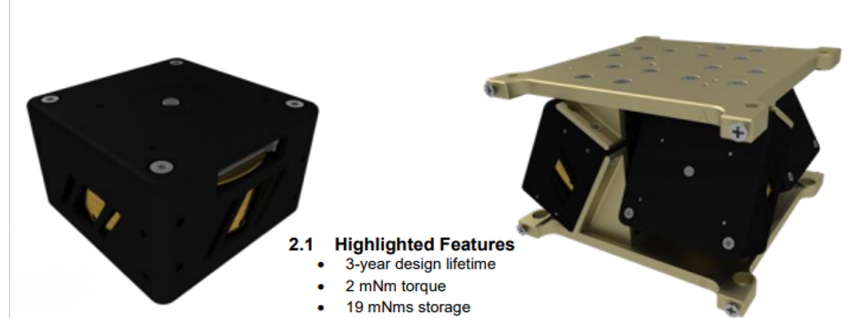
Fig. 3.9. Second option of reaction wheels chosen [34]

- Magnetorquer MTQ400 by Hiperion Technologies

Specifications
- Available as MTQ400.50 or MTQ400.40
- Includes drive electronics
- Nominal dipole moment: 0.5 / 0.4 A.m²
- Boost mode dipole moment: up to 2 Am² / up to 1.5 A.m²
- Dimensions: 11.5 x 80 mm / 11.5 x 65 mm (Ø x l)
- Mass: 44.1 / 34.5 g
- Dipole moment directly controllable, in steps of 1 mA.m²
- Power consumption at nominal dipole moment only 270 / 350 mW
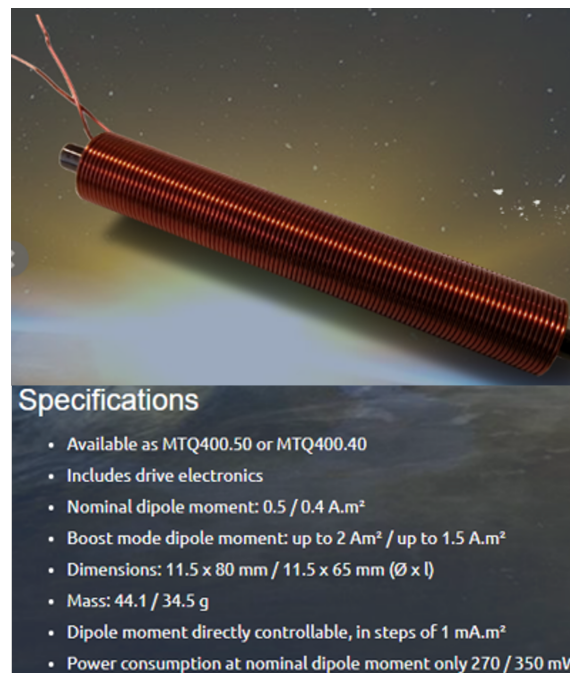
Fig. 3.10. First option of magnetorquers chosen [11]

This first option is more adjusted to the 0,63 A^2 value first estimated. With the boost

mode the value needed could be reaches, so in further stages of the design one of the two options should be chosen, MTQ400.50 or MTQ400.40.

- Magnetorquer NCTR-M012 by New Space systems

	NCTR-M012
FUNCTIONAL CHARACTERISTIC	
Magnetic moment	1.19 Am²
Linearity (across operating range)	<± 5%
Residual moment	<0.005 Am²
PHYSICAL CHARACTERISTICS	
Dimensions (l x w x h)	94 mm x 15 mm x 13 mm
Mounting feet	2
Mass	<50 g
Power	<800 mW nominal @ 5 V

Fig. 3.11. Second option of magnetorquers chosen [12]

This second option may be a bit oversized but would probably reduce the time needed for desaturation.

Considering the two pair of options for reaction wheels and magnetorquers, the following options are possible:

$T_{MT}(mNm)$	Desaturation Time (min)	ReactionWheel GOMSPACE	ReactionWheel BLUE CANYON
0,05	MTQ400.40	8,4	6,7
0,03	NCTR-M012	10,6	8,3
	H(mNms)	19	15
	t until Desaturation (min)	113,5	89,6
	Orbits until Desaturation	1,2	0,95
	Size (cm)	44X44X27	42X42X19

Table 3.3. REACTION WHEELS AND MAGNETORQUERS
PERFORMANCES

Considering the data shown in Table 3.3, the option of the GS600 with any of the magnetorquers would comply with the 1 full orbit pointing need with a 20 % margin. Desaturation time using whichever magnetorquer (MTQ400.4 or NCTR-M012) represents a maximum of less than 11 minutes, which is a bit more than an 11 % of the orbit time. This seems to be reasonable, provided that the real desaturation time would be greater if

more than 1 reaction wheel need to be desaturated at the same time or in short periods of time. More detail analysis would be needed when developing the GNC software of the Desaturation Mode.

3.4.2. Sensors

In order to determine the sensors to be mounted in the satellite, position and pointing requirements must be taken into account

On board computer (OBC)

For this mission, in the frame of the Madrid Flight On Chip Program (see Reference [35]), the OBC Zynq-7000 family or better are to be used (Figure 3.12) as first option.

Further study should be carried out on the magnetic dipole this system would induce in the satellite, targeting the 0.2 Am^2 as explained beforehand. Apart from that, the level of radiation absorbed by the computer during the mission should also be considered as this is a non-space prepared OBC that would require specific protection.

- Zynq-7000 by Xilinx

Zynq-7000 SoC First Generation Architecture

The Zynq®-7000 family is based on the Xilinx SoC architecture. These products integrate a feature-rich dual-core or single-core ARM® Cortex™-A9 based processing system (PS) and 28 nm Xilinx programmable logic (PL) in a single device. The ARM Cortex-A9 CPUs are the heart of the PS and also include on-chip memory, external memory interfaces, and a rich set of peripheral connectivity interfaces.

Processing System (PS)

ARM Cortex-A9 Based Application Processor Unit (APU)
- 2.5 DMIPS/MHz per CPU
- CPU frequency: Up to 1 GHz
- Coherent multiprocessor support
- ARMv7-A architecture
  - TrustZone® security
  - Thumb®-2 instruction set
- Jazelle® RCT execution Environment Architecture
- NEON™ media-processing engine
- Single and double precision Vector Floating Point Unit (VFPU)
- CoreSight™ and Program Trace Macrocell (PTM)
- Timer and Interrupts
  - Three watchdog timers
  - One global timer
  - Two triple-timer counters

Caches
- 32 KB Level 1 4-way set-associative instruction and data caches (independent for each CPU)
- 512 KB 8-way set-associative Level 2 cache (shared between the CPUs)
- Byte-parity support

On-Chip Memory
- On-chip boot ROM
- 256 KB on-chip RAM (OCM)
- Byte-parity support

External Memory Interfaces
- Multiprotocol dynamic memory controller
- 16-bit or 32-bit interfaces to DDR3, DDR3L, DDR2, or LPDDR2 memories
- ECC support in 16-bit mode
- 1GB of address space using single rank of 8-, 16-, or 32-bit-wide memories
- Static memory interfaces
  - 8-bit SRAM data bus with up to 64 MB support
  - Parallel NOR flash support
  - ONFI1.0 NAND flash support (1-bit ECC)
  - 1-bit SPI, 2-bit SPI, 4-bit SPI (quad-SPI), or two quad-SPI (8-bit) serial NOR flash

8-Channel DMA Controller
- Memory-to-memory, memory-to-peripheral, peripheral-to-memory, and scatter-gather transaction support

I/O Peripherals and Interfaces
- Two 10/100/1000 tri-speed Ethernet MAC peripherals with IEEE Std 802.3 and IEEE Std 1588 revision 2.0 support
  - Scatter-gather DMA capability
  - Recognition of 1588 rev. 2 PTP frames
  - GMII, RGMII, and SGMII interfaces
- Two USB 2.0 OTG peripherals, each supporting up to 12 Endpoints
  - USB 2.0 compliant device IP core
  - Supports on-the-go, high-speed, full-speed, and low-speed modes
  - Intel EHCI compliant USB host
  - 8-bit ULPi external PHY interface
- Two full CAN 2.0B compliant CAN bus interfaces
  - CAN 2.0-A and CAN 2.0-B and ISO 118981-1 standard compliant
  - External PHY interface
- Two SD/SDIO 2.0/MMC3.31 compliant controllers
- Two full-duplex SPI ports with three peripheral chip selects
- Two high-speed UARTs (up to 1 Mb/s)
- Two master and slave I2C interfaces
- GPIO with four 32-bit banks, of which up to 54 bits can be used with the PS I/O (one bank of 32b and one bank of 22b) and up to 64 bits (up to two banks of 32b) connected to the Programmable Logic
- Up to 54 flexible multiplexed I/O (MIO) for peripheral pin assignments

Interconnect
- High-bandwidth connectivity within PS and between PS and PL
- ARM AMBA® AXI based
- QoS support on critical masters for latency and bandwidth control

Fig. 3.12. OBC Zynq-7000 [13] as proposed for Madrid Flight On Chip [35]

However, since this is an experimental program whose feasibility is still to be confirmed, an alternative OBC has been chosen. This one, as shown in Figure 3.13, is a flight-proven computer that also has a 3-axis gyroscope and a 3-axis magnetometer, whose versatility will provide redundancy with little power and space budget costs, ideal for a small satellite as it is the case.

- A3200 NanoMind

NanoMind A3200

Datasheet
On-board Computer System for mission critical space applications

2 Overview
The NanoMind A3200 (A3200) contains three main parts.

- The A3200 on-board computer (OBC) is designed as an efficient system for space applications with limited resources, such as e.g. for CubeSat or nano-satellite missions.
- A 3-Axis magnetometer and coil-drivers that can be used to implement attitude control based on magnetic sensing and actuation.
- A 3-Axis gyroscope used for attitude control.

Its main interface to other subsystems is CAN and I²C. For storage, the board carries a 128 MB NOR serial flash. The RTC chip on the board also functions as a processor companion while 32 kB of FRAM provides non-volatile storage.

Beside the I²C controller for the main bus the board also has an extra I²C controller that can be used to interface to external I²C components. For interfacing with SPI devices, the board has one external connection with three chip selects. Furthermore, it has 8 inputs to an ADC. If needed, the ADC inputs can also be used as GPIO.

The form factor of the A3200 fits on the GomSpace NanoDocks, which makes it possible to fit both the A3200 and another daughterboard next to each other in the same space as a standard OBC would require.

2.1 Highlighted Features
- High-performance AVR32 MCU with advanced power saving features
- Clock frequency from 8 MHz to 64 MHz
- 512 KB build-in flash
- IEEE 754 FPU
- Wide range for clocks speeds with build-in PLL
- Multiple CSP data interfaces: I²C, UART, CAN-Bus
- 128 MB NOR flash (On two dies of 64 MB each)
- 32 kB FRAM for persistent configuration storage
- 32 MB SDRAM
- RTC clock
- On-board temperature sensors
- 8 external ADC channels that also can be used as GPIO
- External SPI with 3 chip selects
- Attitude stabilization system
    - 3-Axis magneto resistive sensor
    - 3-Axis gyroscope
    - 3 bidirectional PWM outputs with current measurement
    - I²C interface for GomSpace Sensor Bus (GSSB)

Fig. 3.13. OBC A3200 NanoMind by Gomspace [36]

GPS receiver and antenna

As a constraint to set the GPS receiver and antenna, the accuracy of 10 m RMS when determining the spacecraft position must be taken into account. This requirement comes from the MarinLara mission R-M0-MIS-030 as stated in [29]. Thus, the following components by New Space Systems were chosen:

CUBESAT GPS RECEIVER		NANT-PTCL1	
FUNCTIONAL CHARACTERISTICS		**FUNCTIONAL CHARACTERISTICS**	
Position accuracy [1σ]	<10 m	Frequency	1575.42 MHz
Velocity accuracy [1σ]	<25 cm/s	Bandwidth	20 MHz
Update rate	1 Hz	-3 dB beamwidth	≥100° (phi = 0°); ≥100° (phi = 90°)
Operating frequency	L1 (1575.42 MHz)	Return loss	≤-5 dB
PHYSICAL CHARACTER		Impedance	50 Ohm (matched)
		Active gain (RHC)	≥16 dBi
Dimensions	96 mm x 96 mm x 15 mm	Polarization	Right Hand Circular (RHCP)
Mass	<110 g	Noise figure	<2 dB
Power	1 W (excluding active antenna)	Axial Ratio	<4 dB
ENVIRONMENTAL CHA		**PHYSICAL CHARACTERISTICS**	
Thermal (operational)	-10 °C to +50 °C	Dimensions	54 mm x 54 mm x 14.1 mm
Vibration (qualfication)	14 g_{RMS} (random)	Mass	<80 g
Radiation (TID)	10 krad (component level)	Power	<80 mW
INTERFACES		**ENVIRONMENTAL CHARACTERISTICS**	
Power supply	5 V_{DC} and 3.3 V_{DC}	Thermal (operational)	-25 °C to +55 °C operating, -30 °C to +60 °C non-operating
Data	RS-422 UART	Vibration (qualification)	14 g_{RMS} (random)
		Radiation (TID)	10 krad (component level)
Connector	PC 104	**INTERFACES**	
		Power supply	5 V_{DC} nominal
		Connector	50 Ω SMA female
Mechanical	CubeSat PC 104 form factor	Mechanical	4 x M3 through hole

Fig. 3.14. Cubesat GPS receiver and NANT-PTCL1 GPS antenna [15]

The accuracy target is exactly the one that provide these components and other deviations, such as thermal deformations and mounting misalignment are not comparable to these 10 m for a satellite of the dimensions given in this case.

Magnetometer (MM)

The magnetorquers that will desaturate the reaction wheels need to know the intensity and direction of the magnetic field they are suffering for the AOCS control to determine how to actuate them to compensate the unwanted torque from the reaction wheels desaturating. Consequently, a 3 axis magnetometer or an Earth magnetic field model should be installed in the spacecraft.

In order to be conservative in terms of power and space/mass need, the option of a magnetometer is analyzed. After a benchmarking process (OCE Tecnology [37], Meisei [38], Antrix [39]) it was noted that the the maximum accuracy that can be reached is around degree. Then, 2 options of magnetometer have been chosen.

- One from New Space Systems, model NMRM-001-485, since several COTS pro-

posed where from this supplier and this could imply certain facilities and less cost when finally purchasing them. Furthermore, the range of magnetic field that the device can measure, up to 6 Gauss is big enough to cover the range of magnetic field expected during the operation of the spacecraft, as can be inferred from Figures 3.6 and 3.7.

	NMRM-001-485
FUNCTIONAL CHARACTERISTICS	
Orthogonality	<+/- 1 degree
Measurement range	-60,000 nT to +60, 000 nT
Resolution	<8 nT
Update rate	<18 Hz
Noise density	<8 nT rms/Hz @ 1 Hz
PHYSICAL CHARACTERISTICS	
Dimensions	96 mm x 45 mm x 20 mm
Mass	<67 g
Power	<550 mW
ENVIRONMENTAL CHARACTERISTICS	
Thermal (operational)	-25 °C to +70 °C
Vibration (qualfication)	14 g_{RMS} (random)
Radiation (TID)	10 krad (component level)
INTERFACES	
Power supply	5 V_{DC}
Data	RS-485
Connector	15-pin Female Micro-D
Mechanical	4off M3

Fig. 3.15. NMRM-001-485 magnetometer [17]

- The other one, from Honeywel, model HMC5843, is integrated inside the on board computer and, as explained before, this represents a cost and volume savings source. In this case, again, the magnetometer covers the full range of 6 gauss magnetic field to be measured and power need is much lower, 3 mW as compared to the 550 mW of the NewSpace option.. However, accuracy is much lower in this case, with a resolution of 700 ηT, as compared with the 8 ηT of the previous option.

HMC5843 3-Axis Acceleration Sensor **Honeywell**

3-Axis Magneto resistive Sensors and ASIC in a Single Package

Small Size for Highly Integrated Products. Just Add a Micro-Controller Interface, Plus Two External SMT Capacitors

Low Cost

Designed for High Volume, Cost Sensitive OEM Designs

4.0 x 4.0 x 1.3mm Low Height Profile LCC Surface Mount Package

Easy to Assemble & Compatible with High Speed SMT Assembly

Low Voltage Operations (2.5 to 3.3V)

Compatible for Battery Powered Applications

Built-In Strap Drive Circuits

Set/Reset and Offset Strap Drivers for Degaussing, Self Test, and Offset Compensation

I2C Digital Interface

Popular Two-Wire Serial Data Interface for Consumer Electronics

Lead Free Package Construction

Complies with Current Environmental Standards

Wide Magnetic Field Range (+/-6 Oe)

Applications:

- Compassing
- Magnetometer

Fig. 3.16. HMC5843 magnetometer [40]

However, it must be noted that no magnetometer may be used if the interaction between the magnetorquer and this device makes the magnetic field measurements useless. Consequently, a magnetic field model could be loaded in the memory of the satellite instead.

Sun sensors

The purpose of installing sun sensors in the satellite, in this case, is providing the system with a more robust, although less accurate, attitude sensor for the safe mode. Fine sensors have been considered as a conservative measure to take into account those sensors that are more performing if needed, and consequently, bigger and with more power need.

Two different models have been proposed:

- NFSS-411 by New Space systems

  With a field of view of 140° and an accuracy of 0.1° RMS, 4 of them would be needed to fully determine the Sun position if they are well positioned. This is a high accuracy Sun Sensor whose need should be duly justified when analysing with detail the safe mode pointing accuracy and robustness needs.

	NFSS-411
FUNCTIONAL CHARACTERISTICS	
Field of view	140°
Update rate	5 Hz
Accuracy	≤ 0.1° RMS error over the FOV
PHYSICAL CHARACTERISTICS	
Dimensions	34mm x 32mm x 20mm
Mass	35g
Power	37.5mW average, 130mW peak
ENVIRONMENTAL CHARACTERISTICS	
Thermal (operational)	-25°C to +70°C
Vibration (qualification)	16.3g RMS random (10g RMS acceptance), 5000g shock
Radiation (TID)	10krad total dose (component level)
INTERFACES	
Power supply	5V DC nominal (5V to 50V)
Data	RS-485 UART
Connector	9-way female Micro-D
Mechanical	4x #2 Socket Head Cap Screw (or M2)

Fig. 3.17. NFSS-411 sun sensor [18]

- Cubesense, Fine Sun or Earth sensor by Cubespace

  It represents an even more performing sensor, with $0.2°$ 3σ accuracy than the previous one (NFSS-411 has an equivalent $0.3°$ 3σ accuracy). Furthermore, this sensor has the ability to track both the Earth or the Sun, depending on the measurement configuration. In that way, if in further stages of the project a change in the attitude determination and control system is needed to track the Earth position directly, this provision would ease the iterating process to converge to a final solution. Apart from that, to be able to track the Sun position no matter the relative position of the satellite with respect to it, 3 CubeSense would be needed, since its Field of view is close to $180°$ ($170°$).
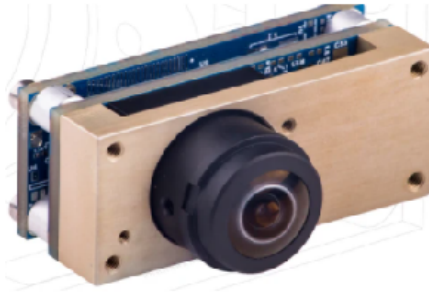
2. Specifications

Table 1 – Performance specifications

Physical	
Size	41.7 x 17.7 x 24.3 mm
Mass	30 g
Power	
Maximum power use	200 mW
Nominal mode	< 100 mW
Performance	
Maximum Update Rate	2 Hz
Accuracy (1σ)	
Nadir option	0.2° (Full earth in FOV)
Sun option	0.2° (Full range)
Detection Range	
Nadir option	130° vertical/horizontal and 160 degrees diagonal
Sun option	170° vertical/horizontal and 180 degrees diagonal

Fig. 3.18. CubeSense, fine Sun or Earth sensor by Cubespace [41]

Pointing budget

In order to select the components needed for attitude determination during the Fine Pointing Mode, these requirements, that were previously considered, are involved:

- Mandatory

  R-M0-ADS-020: Nadir attitude determination by 3 x Nadir antennas shall be known with an accuracy of 0.1 deg with respect to Nadir

- Desirable

  G-M0-ADS-015: Nadir pointing accuracy by 3 x Nadir antennas should be of 0.05°.

Considering such demanding requirements and having revised the State of the art of attitude sensors, as shown in this section, and of the attitude determination and control software, as shown in section 2.5, the attitude hardware considered for the Fine Pointing Mode will be a Star tracker and a gyroscope in a Gyro-stellar Kalman filter configuration, as it is developed in Reference [41].

This Kalmann filter, as a first approximation, can determine the bias errors coming from the gyroscope. This determination leads to consider the noise coming from the star tracker to be "fixed" by the regularity of measures taken by the gyros. Thus, the combination of Star tracker and gyroscope will be considered for the pointing budget as the addition of the bias of the star tracker (different depending on the axis measured), and the low noise remaining from the gyros (bias instability and angular random walk).

Another reason to consider using a star tracker is its ability to provide direct inertial quaternion measurements. Thus, with the use of the GPS to locate the satellite and the Earth, direct attitude determination and pointing towards Nadir can be accomplished.

In order to set a pointing budget of the satellite, as explained in [6], the measurement process with their associated errors have been considered in tables 3.4, 3.5, 3.6 and 3.7. The star tracker measurement error has been taken from the data sheet of the two options considered [21] and [42], using the less accurate measurement direction of the two ($0.061°$ for Cubestar and 30 arcsec = $0.0083°$ for the KU Leuven one). Mounting and attitude determination errors were obtained from [6], page 277, where an example of pointing budget is performed.

The orbit determination error has been estimated through the error in position of the satellite (Velocity error is much lower), coming from the trigonometrical relationship of the distance error with the orbital radius: $\epsilon = atan(\frac{d_{error}}{h_{satellite}})$, where $d_{error} = 30m3\sigma$ is the position accuracy of the GPS, $h_{satellite} = 500km$ is the geometric altitude of the spacecraft over Nadir and ϵ the angular error when pointing to Nadir.

Gyros drift influence on the budget has been calculated as follows, with data from the gyros data sheets:

$$\epsilon_{drift} = \frac{\mu_{Instability_{Gyr}}}{f_{ST}} + \frac{ARW_{Gyr}}{\sqrt{f_{ST}}} \tag{3.11}$$

where $\mu_{Instability_{Gyr}}$ is the bias instability of the gyroscope, ARW_{Gyr} is the angular random walk of the gyroscope and f_{ST} is the sampling frequency of the star tracker (1 Hz for Cubesens and 10 Hz for KU Leuven). This has been assumed due to the fact that the drift of the gyroscope is continuously corrected by the star tracker at the rate it takes measures.

Finally, the instrument alignment error has been considered from the data sheet of the IMU, [20]. However, as it is explained in reference [22], applying a gyro calibration Kalman filter at the start of the mission, the instrument misalignment can be estimated with an error of 2.8% for the most critical alignment matrix element (See page 253 of [22], element k_{L1}). this 97.2% reduction was applied to the initial value of 1 mrad obtained from [20].

All errors where considered to be uncorrelated and 3σ accuracy are in all cases considered.

Considering tables 3.4, 3.5, 3.6 and 3.7, it can be observed that, using the MPU-3300 gyroscopes with the Cubestar star tracker the mandatory requirement is fulfilled, meanwhile with the same gyroscope, the desirable requirement is reached using the KU Luven star tracker. Consequently, the STIM 202 IMU would not be used.

	σ (")	σ(°)	Type (B/R)	Source
Star tracker measurement	219,6	0,061	B	[43]
Gyros drift	20,7	0,0057	R	[21]
Star tracker mounting error	7,2	0,002	R	[6]
Gyros mounting error	7,2	0,002	R	[6]
Instrument alignment	6,9	0,002	B	[19] and [43]
Attitude computation error	0,36	0,0001	B	[6]
Payload mounting error	3,6	0,001	R	[6]
Orbit determination error (Position)	12,4	0,0034	B	[15]
		0,0729	Total	

Table 3.4. POINTING BUDGET FOR CUBESTAR AND MPU-3300 COMBINATION.

	σ (")	σ(°)	Type (B/R)	Source
Star tracker measurement	219.6	0,061	B	[20]
Gyros drift	3,20	0,0009	R	[21]
Star tracker mounting error	7,2	0,002	R	[6]
Gyros mounting error	7,2	0,002	R	[6]
Instrument alignment	6,9	0,001	B	[19] and [20]
Attitude computation error	0,36	0,0001	B	[6]
Payload mounting error	3,6	0,001	R	[6]
Orbit determination error (Position)	12,4	0,0034	B	[15]
		0,0696	Total	

Table 3.5. POINTING BUDGET FOR CUBESTAR AND STIM 202 COMBINATION.

	σ (")	σ(°)	Type (B/R)	Source
Star tracker measurement	30	0,0083	B	[22]
Gyros drift	7,2	0,002	R	[21]
Star tracker mounting error	7,2	0,002	R	[6]
Gyros mounting error	7,2	0,002	R	[6]
Instrument alignment	6,9	0,002	B	[20] and [21]
Attitude computation error	0,36	0,0001	B	[6]
Payload mounting error	3,6	0,001	R	[6]
Orbit determination error (Position)	12,4	0,0034	B	[15]
		0,0174	Total	

Table 3.6. POINTING BUDGET FOR KU LEUVEN AND MPU-3300 COMBINATION.

	σ (")	σ(°)	Type (B/R)	Source
Star tracker measurement	30	0,0083	B	[22]
Gyros drift	2,9	0,0008	R	[21]
Star tracker mounting error	7,2	0,002	R	[6]
Gyros mounting error	7,2	0,002	R	[6]
Instrument alignment	6,9	0,002	B	[20] and [21]
Attitude computation error	0,36	0,0001	B	[6]
Payload mounting error	3,6	0,001	R	[6]
Orbit determination error (Position)	12,4	0,0034	B	[15]
		0,0169	Total	

Table 3.7. POINTING BUDGET FOR KU LEUVEN AND STIM 202 COMBINATION.

Gyroscopes (Gyros)

To complete the previous pointing budgets, the following gyroscopes were selected:

- Sensonor ButterflyGyro^{TM} STIM202 3-Axis Gyro Module.

  This is a more performing and power consuming option, with acceloremeters included, whose utilisation would be justified to target the desirable requirement of 0.05 ° attitude determination accuracy.

Table 6-2: Functional specifications

Parameter	Conditions	Min	Nom	Max	Unit	Note
GYRO						
Full Scale (FS)			±400		°/s	1
Resolution			24		bits	
			0.22		°/h	
Scale Factor Accuracy			±0.2		%	
Non-Linearity	±250°/s		25		ppm	2
	±400°/s		50		ppm	2
Bandwidth (-3dB)			262		Hz	3
Group Delay			1.6		ms	4
Compensation time, t_{comp}	Ref: Figure 8-4	0.78	0.83	0.91	ms	5
Bias Accuracy		-250	0	+250	°/h	
Bias error over temperature	$\Delta T \leq \pm 1°C/min$		30		°/h rms	6
Bias Instability	Root Allan Variance @25°C		0.4		°/h	
Angular Random Walk	Root Allan Variance @25°C		0.15		°/√h	
Linear Acceleration Effect			14		°/h /g	7
Vibration Rectification Coefficient	f<1000Hz		0.1		°/h /g²$_{rms}$	
Misalignment			1		mrad	8

TEMPERATURE MEASUREMENT

ButterflyGyro™

STIM202 3-Axis Gyro Module

(38.6mm x 44.8mm x 20.0mm)

Fig. 3.19. Sensonor ButterflyGyro^{TM} $STIM$ 202 $3-Axis$ $Gyro$ $Module$ $specifications$[20]

- MPU-3300 Gyroscope integrated within Nanomind 3200 on board computer.

   This is a less accurate gyroscope whose main advantage is that it is integrated together with the On board computer. As can be seen in tables 3.4, 3.5, 3.6 and 3.7, the influence of the accuracy of the gyroscope is not critical for attitude determination performance. What makes the difference is the worst axis accuracy of the star tracker. Thus, a more accurate gyroscope would only be needed if the desirable requirement would be targeted, considering that the power consumption of this gyroscope is much lower than that of figure 3.19 (12 mW compared to 1.5 W).

MPU-3300 Product Specification Revision 1.0

GYROSCOPE NOISE PERFORMANCE	FS_SEL=0				
Total RMS Noise	DLPFCFG=2 (100Hz)		0.05		°/s-rms
Low-frequency RMS noise	Bandwidth 1Hz to10Hz		0.033		°/s-rms
Rate Noise Spectral Density	At 10Hz		0.005		°/s/ √Hz
GYROSCOPE MECHANICAL FREQUENCIES					
X-Axis		30	33	36	kHz
Y-Axis		27	30	33	kHz
Z-Axis		24	27	30	kHz
LOW PASS FILTER RESPONSE					
	Programmable Range	5		256	Hz
OUTPUT DATA RATE					
	Programmable	4		8,000	Hz

7.10 Bias Instability

Bias Instability is a critical performance parameter for gyroscopes. The MPU-3300 provides typical bias instability of 15°/hour on each axis, measured using the Allan Variance method. The figures below show

Fig. 3.20. MPU-3300 Gyroscope specifications [43]

Star tracker

If the mandatory pointing requirement needed is to be complied with, a star tracker of the type shown in figure 3.21, must be mounted in the satellite. This is the case because the roll determination accuracy of the device is not high enough to comply with the requirement imposed, having the instrument misalignment considered.

Physical	
Mass	55g
Dimensions	50 x 35 x 55 mm
Operating temperature	-10°C to 60°C
Vibration	8.03 g RMS random (lens supported)
Electrical	
Supply voltage	3V3
Average power	<142mW
Peak power	<264mW
Communications	I2C/UART
Performance	
Accuracy (3-sigma)	
— Cross-axis (RA)	<0.0154°
— Cross-axis (DE)	<0.0215°
— Roll	<0.061°

Fig. 3.21. CubeStar star tracker by CubeSpace [21]

Another option is to select the KU Leuven star tracker, as shown in figure 3.22. This one is a more performing one that would target the desirable attitude determination requirement of 0.05°.
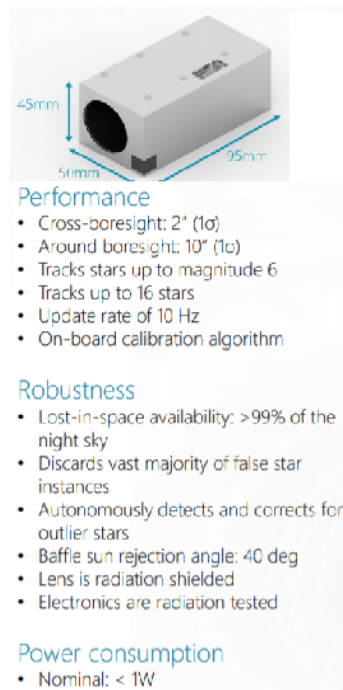

Fig. 3.22. KU Leuven Star tracker [42]

3.4.3. AOCS architecture discussion

The target is to obtain two configurations of the ADCS, one that fulfills the mandatory requirements and one for the desirable ones. In that way, the only difference needed is to change the star tracker to be mounted, as discussed in the previous section.

Modes hardware configuration, mass, volume, power and cost budgets

In order to be able to develop the functionalities assigned to each mode, Table 3.8 summarizes the usage of each component per mode.

	Model	Supplier	Number	SBM	SM	FPM	DsM	DtM	EM
Reaction Wheels	GSW600	Gomspace	3		X	X	X		X
Magnetorquer	MTQ400	Hyperion Technologies	3				X	X	
Star tracker	KU Leuven/ CubeStar	Leuven/ CubeSpace	1			X			
OBC+IMU	Nanomind A3200	Gomspace	1	X	X	X	X	X	X
Sun Earth Sensor	CubeSense	Cubespace	3		X				
GPS Receiver	NGPS-Cubesat Receiver	NewSpace Systems	1	X	X	X	X	X	X
GPS Antenna	NANT-PTCL1	NewSpace Systems	1	X	X	X	X	X	X

Table 3.8. MODES HARDWARE COMPONENTS

As it can be observed, the star tracker will be operating only due to the Fine Pointing mode due to power restrictions limnits, as it will be observed in Tables 3.12 and 3.11. Reaction wheels will always be operating except in the detumbling mode, when only the magnetorquers will be in charge of reducing the uncontrolled satellite angular velocity gained after its deployment. Magnetorquers will also be operating in the desaturation mode when reaction wheels reach the saturation limit. Sun/Earth sensor will only be used when safe mode needs to be operated. In nominal conditions, only after the first detumbling, this safe mode would be needed.

Regarding the number of components needed, as it was discussed in previous sections:

- Three reaction wheels will be used, one per body axis. Although this makes redundancy null, has been consider for the sake of simplicity and affordability in terms of power, as these are design principles for cubesats.

- Three non parallel magnetorquers (see figure 3.23) are forcefully needed in order to be able to develop actuation torque no matter the attitude of the satellite. The reason for this is that magnetic field lines are a quasi-dipole, with almost nule azhimutal component.

- Three Sun/Earth sensors in orther to track the sun in all directions no matter the satellite´s attitude

- One component of each of the others (OBC, ST, GPS), since no redundancy is required.

Regarding the mass and volume budgets shown in Tables 3.10 and 3.9, it can be observed that the ratio between total mass and total volume with margins is below the theoretical limit of 1.33 kg/U (0.94 kg/U for the low performance configuration and 0.98 kg/U for the high performance one). Regarding the total volume occupied, a 1 U target was

called by the ML mission integrator. An excess of 0.5 units is obtained theoretically.

In order to check it, the integration of components in a typical 6U satellite structure has been carried out as can be seen in Figure 3.23. In this approach it can be observed that 2 Us are parcially occupied in the high performance configuration, as estimated in Table 3.10. In the final integration, space optimization could be carried out to reduce the 0.5 extra occupation happening.

Regarding the power needs, a target of 5W was considered by the mission integrator. As observed in tables 3.12 and 3.11, this target is surpassed in SM, FPM, DsM and EM only if the peak power is considered. Consequently, two main actions shall be taken:

1. In further stages of the design, analyze the peak power of each component, typically related to start process, and control the successive switch on to avoid power shortage.

2. Look for other reaction wheels, which are the main power consumption source.

A hardware cost assessment has also been carried out, as can be seen in Table 3.13. With this reference, the mission integrator could evaluate the economical impact that the stringent pointing requirements needed, impose and act in consequence.

Items	Number	Model	Supplier	Unit mass (kg)	Mass (kg)	Width (cm)	Length (cm)	Height (cm)	Unit Volume (Us)	Volume (Us)	Effective Volume (Us)	Volume SF
Reaction Wheels	3	GSW600	Gomspace	0.18	0.54	4.4	4.4	2.7	0.052	0.157	0.235	1.5
Reaction Wheels Support	1	-	Gomspace	0.06	0.06	9.5	9.5	6.16	0.556	0.556	0.834	
Magnetorquer	3	MTQ400	Hyperion Technologies	0.0441	0.1323	1.15	1.15	6.5	0.009	0.026	0.039	
Star tracker	1	CubeStar	Cubespace	0.055	0.055	5	3.5	5.5	0.096	0.096	0.241	
Sun Earth Sensor	3	CubeSense	Cubespace	0.03	0.09	4.17	1.77	2.43	0.018	0.054	0.081	
GPS Receiver	1	NGPS-Cubesat Receiver	NewSpace Systems	0.11	0.11	9.6	9.6	1.5	0.138	0.138	0.207	
GPS Antenna	1	NANT-PTCL1	NewSpace Systems	0.08	0.08	5.4	5.4	1.41	0.041	0.041	0.062	
OBC+Gyroscope	1	Nanomind A3200	Gomspace	0.024	0.024	4.0	6.5	0.7	0.018	0.018	0.027	
				Total mass (kg)	**1.4023**				**Total Volume (Us)**	**0.93**	**1.49**	

Table 3.9. MASS AND VOLUME BUDGET FOR LOW
PERFORMANCE ATTITUDE DETERMINATION CONFIGURATION

Items	Number	Model	Supplier	Unit mass (kg)	Mass (kg)	Width (cm)	Length (cm)	Height (cm)	Unit Volume (Us)	Volume (Us)	Effective Volume (Us)	Volume SF
Reaction Wheels	3	GSW600	Gomspace	0.18	0.54	4.4	4.4	2.7	0.052	0.157	0.235	1.5
Reaction Wheels Support	1	-	Gomspace	0.06	0.06	9.5	9.5	6.16	0.556	0.556	0.834	
Magnetorquer	3	MTQ400	Hyperion Technologies	0.0441	0.1323	1.15	1.15	6.5	0.009	0.026	0.039	
Star tracker	1	KU Leuven	KU Leuven	0.25	0.25	9.5	4.5	5	0.214	0.214	0.321	
Sun Earth Sensor	3	CubeSense	Cubespace	0.03	0.09	4.17	1.77	2.43	0.018	0.054	0.081	
GPS Receiver	1	NGPS-Cubesat Receiver	NewSpace Systems	0.11	0.11	9.6	9.6	1.5	0.138	0.138	0.207	
GPS Antenna	1	NANT-PTCL1	NewSpace Systems	0.08	0.08	5.4	5.4	1.41	0.041	0.041	0.062	
OBC+Gyroscope	1	Nanomind A3200	Gomspace	0.024	0.024	4.0	6.5	0.7	0.018	0.018	0.027	
				Total mass (kg)	**1.4573**			**Total Volume (Us)**		**1.05**	**1.57**	

Table 3.10. MASS AND VOLUME BUDGET FOR HIGH
PERFORMANCE ATTITUDE DETERMINATION CONFIGURATION

	Nominal Power (W)	Max Power (W)	SBM	SM	FPM	DsM	DtM	EM	
Reaction Wheels	1.8	3.15		1	1	1		1	
Magnetorquer	0.81	1.05				1	1		
Star tracker	1	1.5			1				
OBC+IMU	0.17	0.9	1	1	1	1	1	1	
Sun Earth Sensor	0.3	0.6		1					
GPS Receiver	1	1	1	1	1	1	1	1	
GPS Antenna	0.08	0.08	1	1	1	1	1	1	**MAX (W)**
		TOTAL MAX POWER	1.98	5.73	6.63	6.18	3.03	5.13	**6.63**
		TOTAL NOMINAL POWER	1.25	3.35	4.05	3.86	2.06	3.05	**4.05**

Table 3.11. POWER BUDGET FOR LOW PERFORMANCE
ATTITUDE DETERMINATION CONFIGURATION

	Nominal Power (W)	Max Power (W)	SBM	SM	FPM	DsM	DtM	EM	
Reaction Wheels	1.8	3.15		1	1	1		1	
Magnetorquer	0.81	1.05				1	1		
Star tracker	0.142	0.264			1				
OBC+IMU	0.17	0.9	1	1	1	1	1	1	
Sun Earth Sensor	0.3	0.6		1					
GPS Receiver	1	1	1	1	1	1	1	1	
GPS Antenna	0.08	0.08	1	1	1	1	1	1	**MAX (W)**
		TOTAL MAX POWER	1.98	5.73	5.394	6.18	3.03	5.13	**6.18**
		TOTAL NOMINAL POWER	1.25	3.35	3.192	3.86	2.06	3.05	**3.86**

Table 3.12. POWER BUDGET FOR HIGH PERFORMANCE
ATTITUDE DETERMINATION CONFIGURATION

	Units	Model	Supplier	Unit Price ($)	Unit Price (€)	Price (€)
Reaction Wheels	4	GSW600	Gomspace	44944	40000	40000
Reaction Wheels Support	1	-	Gomspace			
Reaction Wheels	3	GSW600	Gomspace	17978	16000	48000
Reaction Wheels	3	RWP015	Blue Canyon Technologies	10000	8900	26700
Magnetorquer	3	NCTR-M012	NewSpace Systems	2000	1780	5340
Star tracker	1	KU Leuven	KU Leuven	50562	45000	45000
Star tracker	1	CusbeStar	CubeSense	13500	12015	12015
Sun Earth Sensor	4	CubeSense	Cubespace	2950	2625.5	10502
GPS Receiver	1	NGPS-Cubesat Receiver	NewSpace Systems	30000	26700	26700
GPS Antenna	1	NANT-PTCL1	NewSpace Systems	5000	4450	4450
OBC	1	NanoMind A3200	Gomspace	6742	6000	6000
			LOW PERFORMANCE	**TOTAL PRICE (k€)**		153
			HIGH PERFORMANCE	**TOTAL PRICE (k€)**		186

Table 3.13. POWER BUDGET FOR HIGH PERFORMANCE
ATTITUDE DETERMINATION CONFIGURATION

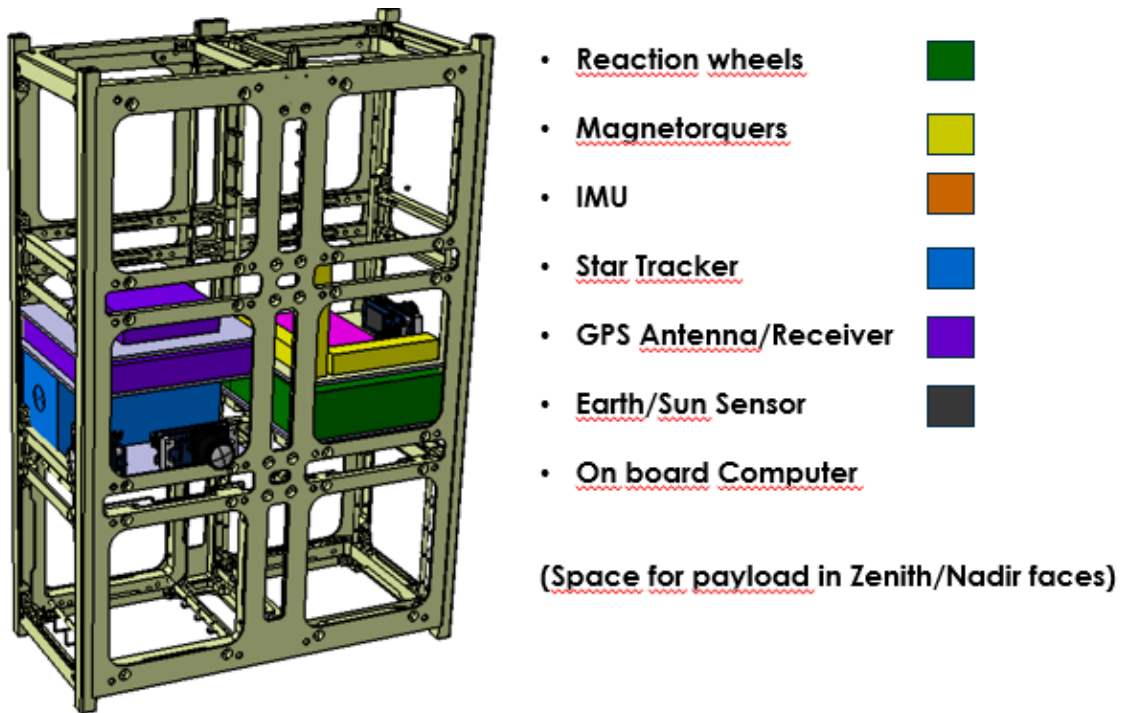Fig. 3.23. High performance attitude determination option components integration

Modes transitions

As part of the modes definition, the in and out conditions must be defined. As can be observed in Figure 3.24, a state machine with one state associated to each mode has been developed.
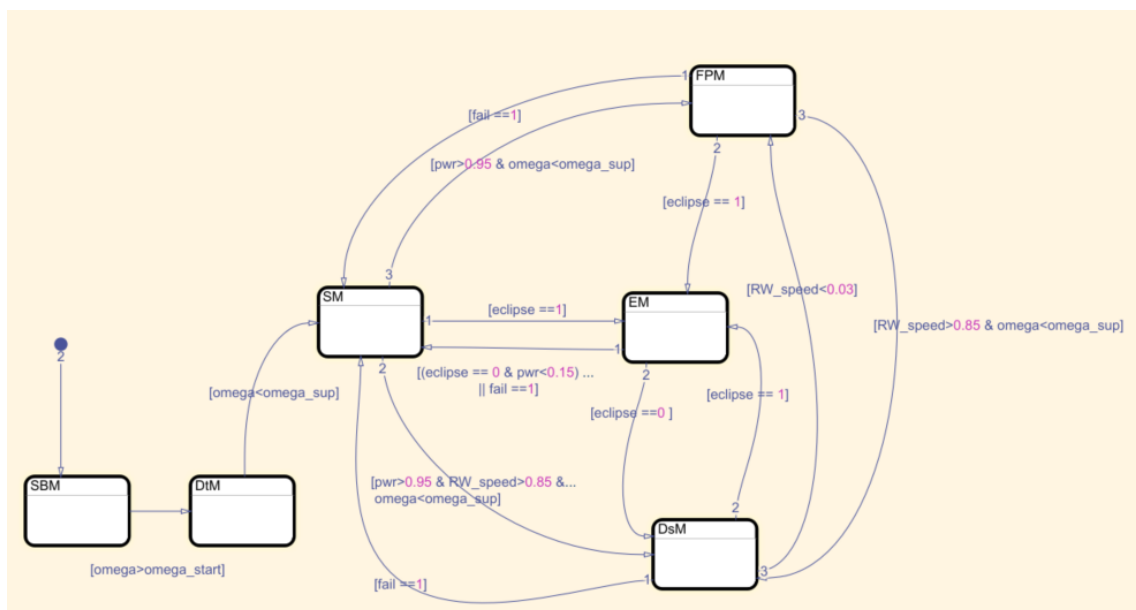

Fig. 3.24. State machine implemented

Observing this figure, the following in and out conditions can be observed:

1. SBM

   - In: Inside launcher
   - Out: Satellite angular speed above a limit o be defined.

2. DtM

   - In: Satellite angular speed above a limit o be defined.
   - Out: Satellite angular speed below a limit o be defined.

3. SM

   - In: Failure or out from DtM or out from EM and power below limit to be defined.
   - Out: When failure is corrected or after battery full charge, after DtM.

4. EM

   - In: Eclipse
   - Out:End of eclipse

5. DsM

   - In: Reaction wheels above limit of saturation and battery level above limit.
   - Out: Reaction wheels below limit of desaturation or failure

6. FPM

   - In: Orbit moment in which the payload may be operated.
   - Out: Wheels saturated or failure

It must be noted that regarding the FPM initiation criteria, the nature of the multi-payload activation will probably need ground commands to take part of the daily work profile of the satellite.

4. AOCS MATLAB AND SIMULINK MODEL DEVELOPMENT

With the purpose of understanding the guidance and navigation concept as well as the close-loop control scheme, Figures 4.1 and 4.2 has been depicted.

In the first one, the successive steps between the guidance (what is the pointing needed), the navigation (what is the real pointing) and the control (what to do to change attitude towards the desired one) is shown. In this image, all the components acting in the system are considered and has an associated process or role.
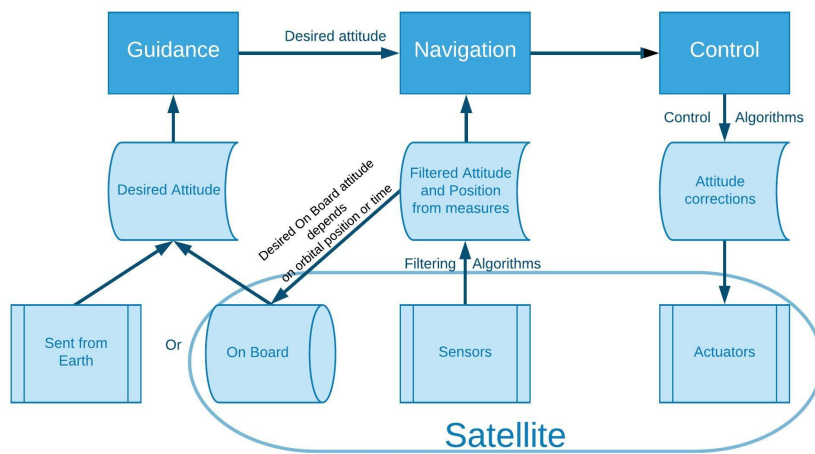
Fig. 4.1. Guidance, navigation and control scheme

In this second one, a more software oriented version of the previous scheme is shown. In it, the relation between the AOCS software and the Dynamics, Kinematics and Environment simulator is shown. This resembles perfectly the software that has been developed as will be seen in the following sections.
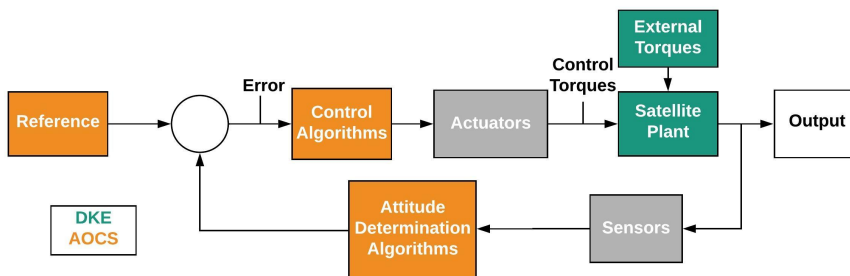
Fig. 4.2. Close control loop scheme

4.1. Initial model description

The first question to determine in this section is what is the scope of the model that has been developed. Due to the resources and time limitations, the full attitude determination and control systems cannot be developed. Then, in order to maximize the utility of the project in the frame of the MartinLara mission, the FPM has been targeted as scope of the thesis. In more detail, the mission phase software regarding guidance, navigation and control has been developed and partially tested to show the feasibility of the mission

For the sake of clarity, description of individual subsystems as per Figure 4.2 is going to be carried out. The reason for these is to ease the interpretation of the images and to avoid none-sense repetition of images.

Another considerations that must be taken is that, all the information related the environment has been modelled and taken from reference [32]. Regarding the spacecraft inertia, values from section 3.3.1 have been selected

4.2. Sensors and actuators modelling

4.2.1. Sensors

Within the scope of the project, both gyroscopes and a star tracker have been modelled as it is explained in the following.

Gyroscope model

As explained in reference [22], the gyroscope basic behaviour can be model as stated in the equations below:

$$\omega = (I_3 + S^{\text{true}})\,\omega^{\text{true}} + \beta^{\text{true}} + \eta_v \tag{4.1}$$

$$\dot{\beta}^{\text{true}} = \eta_{\text{u}} \tag{4.2}$$

where ω is the measured angular velocity, S^{true} is the misalignment matrix, ω^{true} is the real angular speed obtained from the DKE, β^{true} is the gyroscope bias and η_v and η_u are the angular random walk noise and the bias instability or rate random walk, respectively.

This model is implemented as it is shown in Figures 4.3 and 4.4.
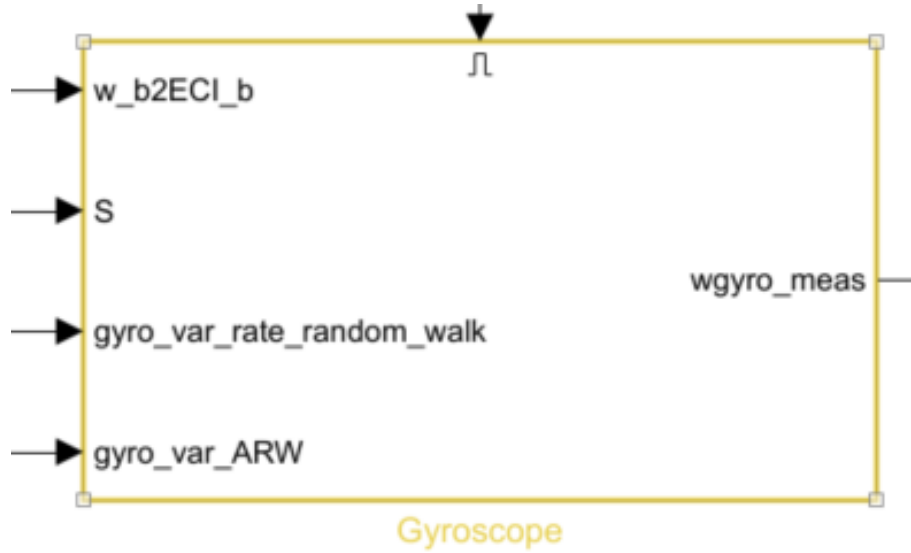
Fig. 4.3. Gyros subsystem with real angular velocity, misalignment matrix and noise (process and bias) inputs
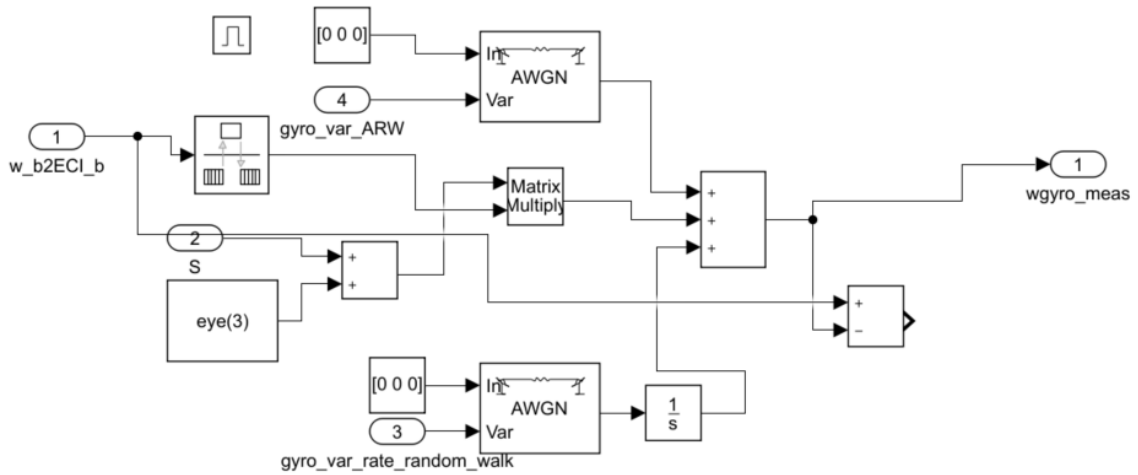
Fig. 4.4. Detailed implementation of the gyroscope model.

Star tracker model

As stated in reference [41], the model of the star tracker can be defined as a multiple quaternion rotation, as shown in equations below:

$$q_{STR}^{SIMULATED} = q_{I \to B} \odot q_{B \to STR} \odot \delta q_{\theta rr}^{STR} \tag{4.3}$$

$$\delta q_{\text{err}}^{STR} = \frac{1}{\sqrt{1 + \frac{\Delta \theta^2}{4}}} \left[\frac{1}{\Delta \bar{\theta}/2} \right] \tag{4.4}$$

where *q* stands for a quaternion, δq is an error quaternion, $\Delta\theta$ is a local 3-angle error, STR is star tracker and B and I are body and inertial reference frame.

This model is implemented as it is shown in Figures 4.5 and 4.6.
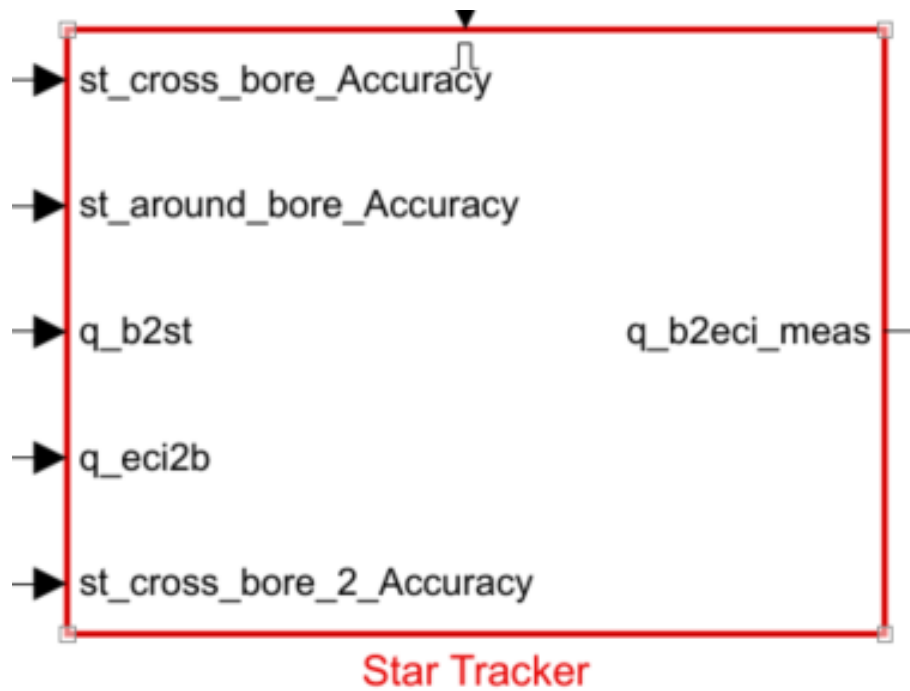
Fig. 4.5. Star tracker subsystem with local angular errors (cross bore, around bore 1 and 2) and body and inertial quaternions as inputs
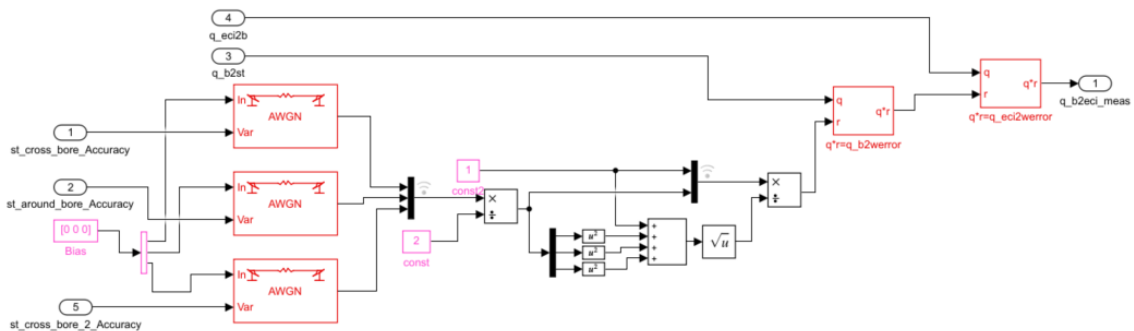
Fig. 4.6. Detailed implementation of the star tracker model.

4.2.2. Actuators

Reaction Wheels

As in this case, only the fine pointing mode is going to be analysed, reaction wheels are the only actuators to be modelled.

In this case, a more applied model has been considered, trying to resemble the torque

and speed curves shown in Figures 4.7 and 4.8from the chosen reaction wheel model from reference [34].
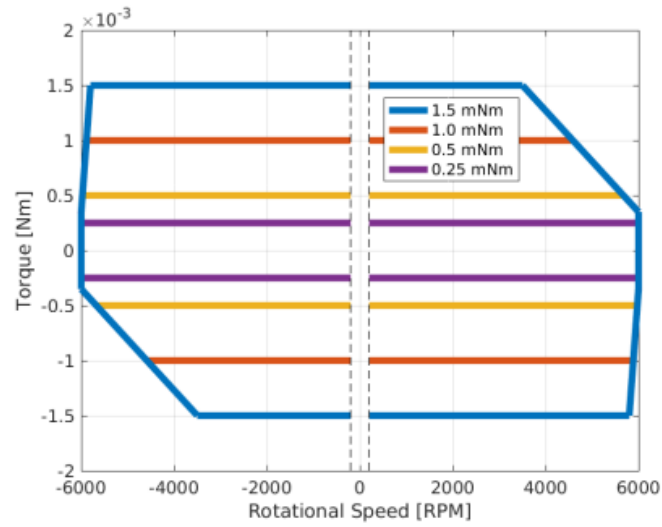
Fig. 4.7. Reaction wheel torque profile [34]s
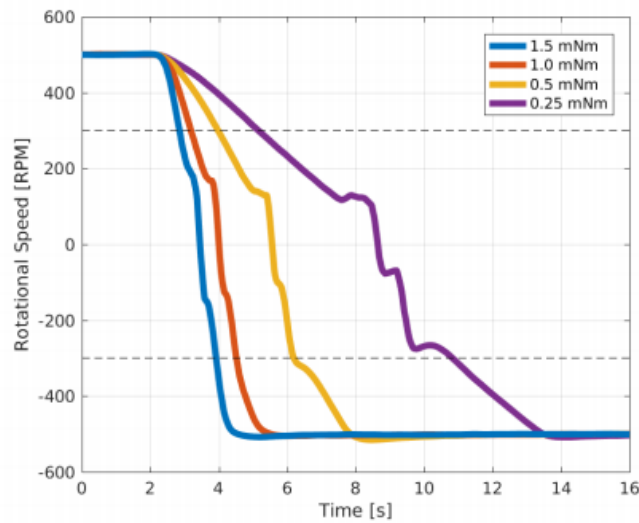
Fig. 4.8. Reaction wheel speed profile [34]ss
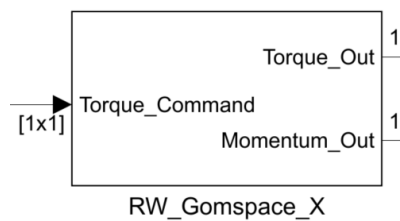
Fig. 4.9. RW subsystem
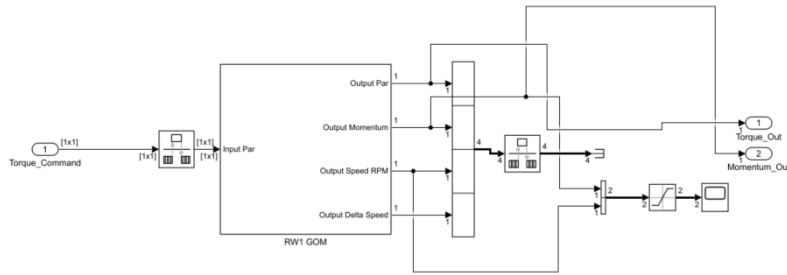
Fig. 4.10. Detailed implementation of the RW model$_1$.
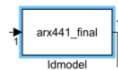
Fig. 4.11. Matlab model to resemble torque and speed cuves.

4.3. GNC modelling

Separated guidance, navigation and control subsystems have been developed:

4.3.1. Guidance

In this case, guidance have been performed through the determination of the quaternion conversion between the Earth Centered Earth Fixed (ECEF) reference frame and the Orbit Reference Frame ORF), taking as references the speed and position measured from the GPS (See figure 4.12. With this information and Earth epehemerides the quaternion between ECEF and body reference frame can be calculated and thus the quaternion error between the desired attitude and the current one.
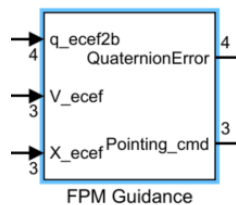
Fig. 4.12. Guidance subsystem
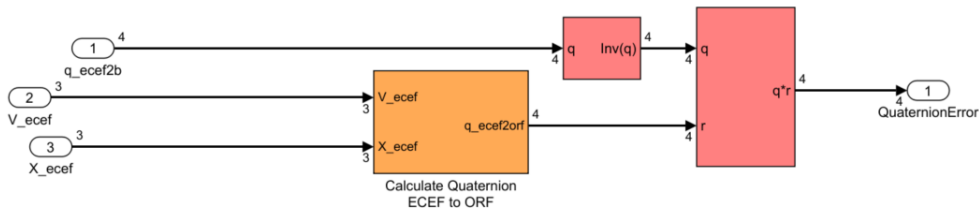
Fig. 4.13. Detailed implementation of the guidance model.
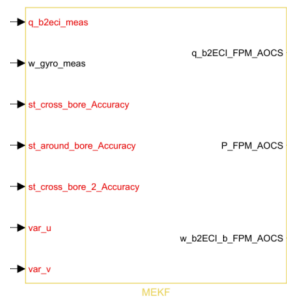
4.3.2. Navigation

Fig. 4.14. Navigation subsystem - Multiplicative extended Kalman filter

The subsystem shown in the image above corresponds to an implementation of the Multiplicative extended Kalman filter algorithm as explained in references [22] and [41]. In this case, a version in which the gyroscope is used as dynamic model replacement is used, as detailed in [41].
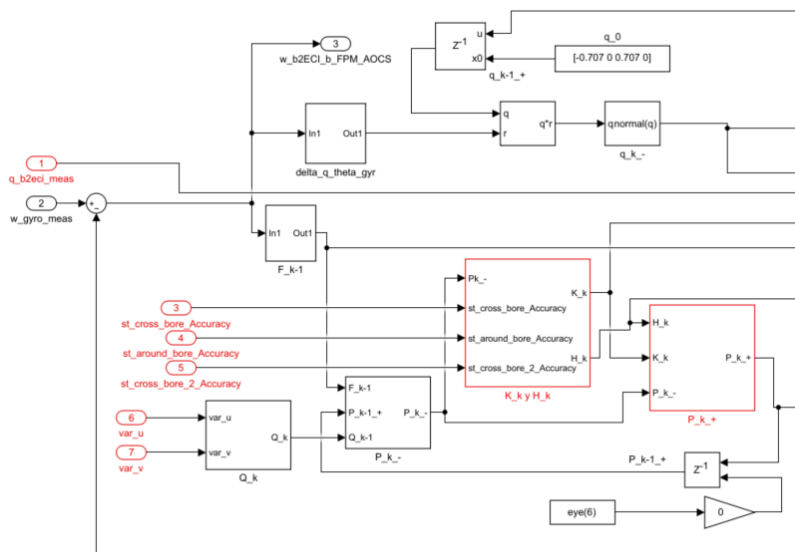
Such implementation can be shown in figures 4.15 and 4.16.

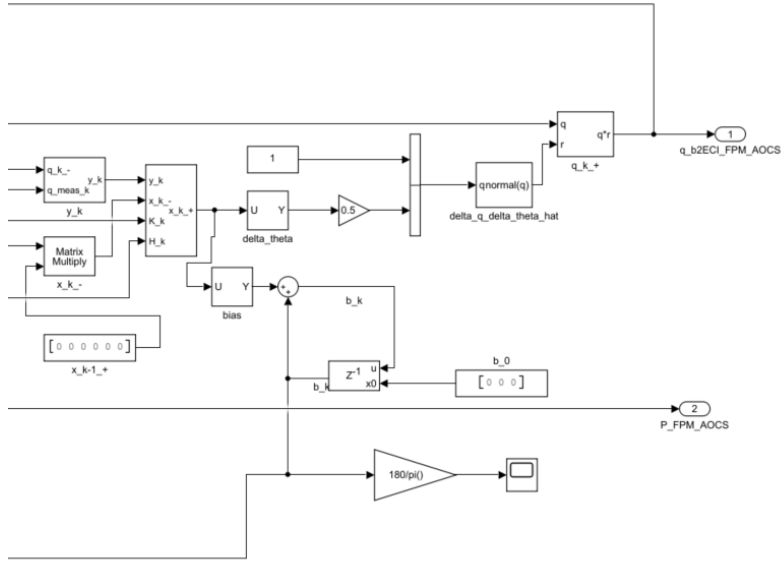Fig. 4.15. Navigation subsystem - Multiplicative extended Kalman filter, detail 1.

Fig. 4.16. Navigation subsystem - Multiplicative extended Kalman filter, detail 2.

The equations that were developed in the model shown above are the following (see reference [22]):

$$\hat{\mathbf{q}}\,(t_0) = \hat{\mathbf{q}}_0, \quad \hat{\beta}\,(t_0) = \hat{\boldsymbol{\beta}}_0$$

$$P\,(t_0) = P_0$$

$$K_k = P_k^- H_k^T \,(\hat{\mathbf{x}}_k^-) \left[H_k\,(\hat{\mathbf{x}}_k^-)\, P_k^- H_k^T\,(\hat{\mathbf{x}}_k^-) + R_k \right]^{-1}$$

$$H_k\,(\hat{\mathbf{x}}_k^-) = \left[\begin{array}{cc} [A\,(\hat{\mathbf{q}}^-)\,\mathbf{r}_1\times] & 0_{3\times3} \\ \vdots & \vdots \\ [A\,(\hat{\mathbf{q}}^-)\,\mathbf{r}_N\times] & 0_{3\times3} \end{array} \right]\Bigg\|_{4\mathbf{k}}$$

$$P_k^+ = [I - K_k H_k\,(\hat{\mathbf{x}}_k^-)]\, P_k^-$$

$$\Delta \hat{\mathbf{x}}_k^+ = K_k \left[\mathbf{y}_k - \mathbf{h}_k\,(\hat{\mathbf{x}}_k^-) \right]$$

$$\Delta \hat{\mathbf{x}}_k^+ \equiv \left[\delta \hat{\vartheta}_k^{+T} \; \Delta \hat{\boldsymbol{\beta}}_k^{+T} \right]^T$$

$$\mathbf{h}_k\,(\hat{\mathbf{x}}_k^-) = \left[\begin{array}{c} A\,(\hat{\mathbf{q}}^-)\,\mathbf{r}_1 \\ A\,(\hat{\mathbf{q}}^-)\,\mathbf{r}_2 \\ \vdots \\ A\,(\hat{\mathbf{q}}^-)\,\mathbf{r}_N \end{array} \right]\Bigg\|_{t\mathbf{k}}$$ (4.5)

$$\hat{\mathbf{q}}^* = \hat{\mathbf{q}}_k^- + \frac{1}{2}\Xi\,(\hat{\mathbf{q}}_k^-)\,8\hat{\vartheta}_k^+$$

$$\hat{\mathbf{q}}_k^+ = \mathbf{q}^* / \|\mathbf{q}^*\|$$

$$\hat{\boldsymbol{\beta}}_k^+ = \hat{\boldsymbol{\beta}}_k^- + \Delta \hat{\boldsymbol{\beta}}_k^+$$

$$\hat{\omega}(t) = \omega(t) - \hat{\boldsymbol{\beta}}(t)$$

$$\dot{\hat{\mathbf{q}}}(t) = \frac{1}{2}\Xi(\hat{\mathbf{q}}(t))\hat{\omega}(t)$$

$$\dot{P}(t) = F(t)P(t) + P(t)F^T(t) + G(t)Q(t)G^T(t)$$

The first 3 are the initial conditions, the next 2 are the Kalman gain calculation and the measurement sensitivity matrix.The last 3 are the dynamic propagation, which in this case is carried out as a direct integration from gyroscope outputs. The other are the state variables update equations. In this case, the state variables are the local angular error $\delta\hat{\vartheta}$ and the gyroscope bias increment $\Delta\hat{\beta}$. As in all the extended Kalman filter, a reference state is taken, first 3 equations, and it is continuously updated with the state variables.

4.3.3. Control

As control algorithm, the solution proposed by Sidi in reference [44]

$$
\begin{aligned}
T_{cx} &= 2K_x q_{1E} q_{4E} + K_{xd} p \\
T_{cy} &= 2K_y q_{2E} q_{4E} + K_{yd} q \\
T_{cz} &= 2K_z q_{3E} q_{4E} + K_{zd} r.
\end{aligned}
\tag{4.6}
$$

where $K_{x,y,z}$ are the proportional gains, $K_{xd,yd,zd}$ are the derivative gains, $q_{1E,2E,3E,4E}$ are the error quaternion components obtained from the MEKF previously explained and p, q, r are the angular speeds obtained also form the MEKF.

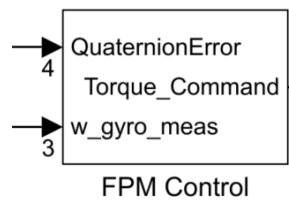These equations implementation is shown in figures 4.17 and 4.18.
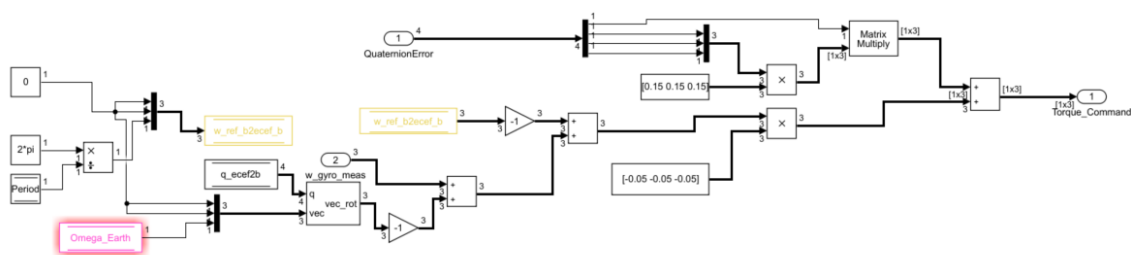

Fig. 4.17. Control subsystem

Fig. 4.18. Detailed implementation of the control model.

5. SIMULATIONS AND CONCLUSIONS

After the previous implementation, the following results and conclusions were gathered.

5.1. Simulations

Considering the separation theorem explained in [22], by which a satellite mission attitude estimation and control algorithms can be separately demonstrated, two main simulations were carried out:

5.1.1. MEKF demonstration

In this case, as can be observed in figure 5.1, in which the MEKF algorithm has been simulated for a polar orbit of 500 km, similar to the one of Martin Lara mission,with the Low performance configuration, the angular determination accuracy is higher than the mandatory requirement of 0.1°, 0.065° in this case, with a convergence time of less than 20 seconds.
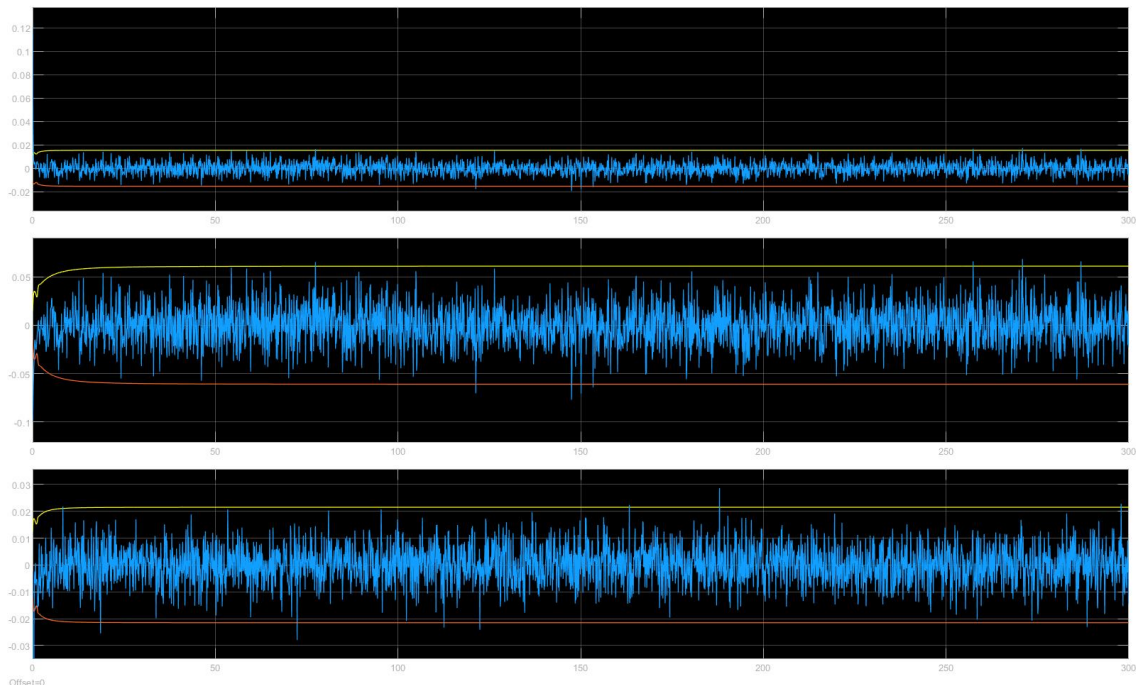

Fig. 5.1. MEKF simulation over 300 seconds. Pitch, roll and yaw angular errors (from top to bottom) in degrees with 3σ accuracy limit over time in seconds.

5.1.2. Control algorithm demonstration

In this case, as can be observed in figure 5.2, in which the control algorithm has been simulated for the Dawn-Dusk orbit of 500 km, the one of the Martin Lara mission, with the Low performance configuration, the angular control accuracy is higher than the mandatory requirement of 1°, 0.15° in this case, with a convergence time of less than 5 minutes. In fact, within the first 90 seconds, the system would already be fulfilling the mandatory requirement regarding control.
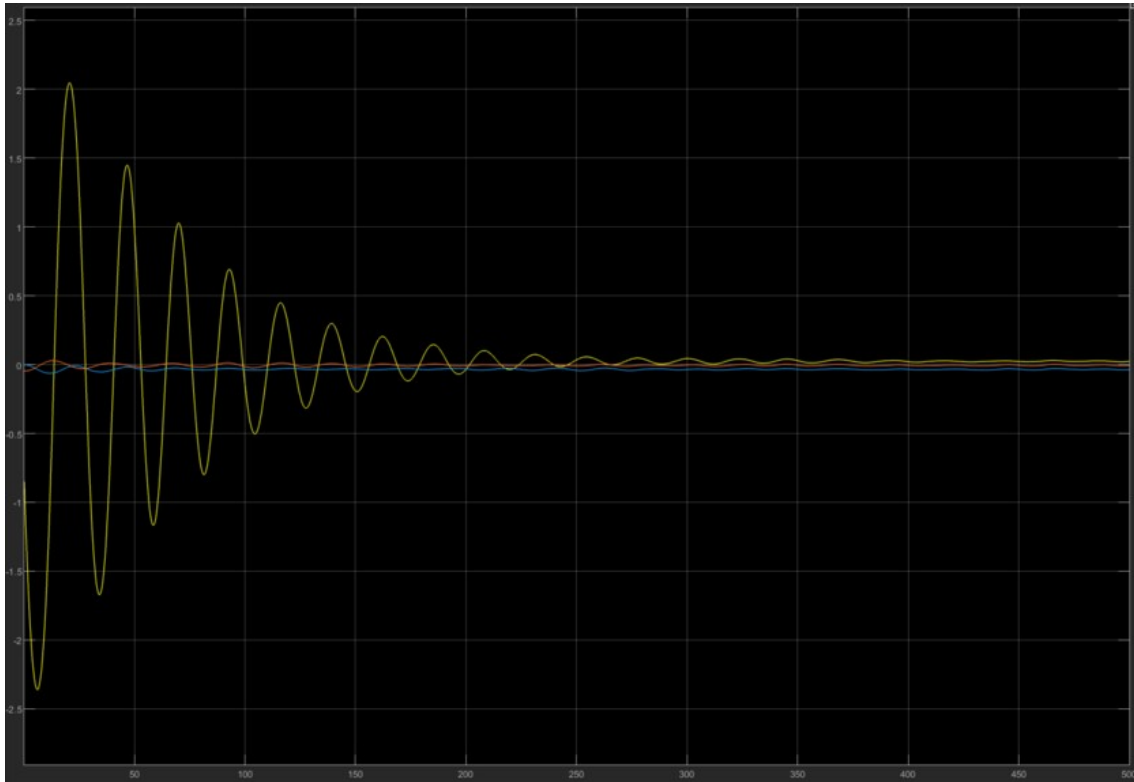

Fig. 5.2. Control algorithm simulation over 500 seconds. Pitch, roll and yaw angular errors (red, yellow, blue) in degrees over time in seconds.

5.2. Conclusions and future steps

5.2.1. Conclusions

After the previous work, from the targeted requirements, the following have been satisfactorily proven with simulations

- R-M0-ADS-010: Nadir pointing accuracy by 3 x Nadir antennas shall be of **1 deg**.

- R-M0-ADS-020: Nadir attitude determination by 3 x Nadir antennas shall be known with an accuracy of 0.1 deg with respect to Nadir.

These requirements have been theoretically demonstrated by analysis:

- R-M0-MIS-030: Absolute position of the spacecraft shall be determined with better accuracy than 10 m (Root Mean Square error).

- R-M2-PYL-170: Measurements with any radiometer pair shall be taken for a complete orbit as a minimum.

- R-M4-PYL-220: The Sun and the Earth penetration in the FOV of each Zenith antenna shall be recorded as a function of time.

- R-M6-MIS-290: The spacecraft shall comply with the Cubesat design standards.

Apart from that, the following requirements have been derived, at least as first approach:

- R-MX-AOCS-010: Magnetic residual dipole of the satellite shall be lower than 0.2 Am° in the pitch body axis.

- R-MX-AOCS-020: MEKF for the commissioning phase shall be able to determine the gyroscope misalignment matrix with a worst accuracy member of 2.8% 3σ.

- R-MX-AOCS-030: The inertia matrix of the final satellite shall be close to the one depicted in section 3.3.1 with a 20% margin.

5.2.2. Future steps

As main future steps to be taken in order to follow the work already started, the following ideas have been fined

1. Test the full complete FPM mission GNC system in several conditions: limit angular speeds, limit angular positions, unknown misalignment... In order to assess roboustness and flexibility.

2. Develop a commanding phase MEKF in order to determine the accuracy with which the system can estimate the gyroscope misalignment.

3. Develop the desaturation GNC software in order to evaluate if the rest of the critical hardware have been properly sized (Magnteorquers essentially).

BIBLIOGRAPHY

[1] P. Fortescue, G. Swinerd and J. Stark. *Spacecraft systems engineering*, 4th ed., Chichester: Wiley, 2011.

[2] M. Herzl. *Estimation of Magnetic Torquing and Momentum Storage Requirements for a Small Satellite*.Undergraduate research Symposium. Colorado Space Grant Symposium, 2010.

[3] Members of the Technical Staff Attitude Systems Operation Computer Science Corporation. *Spacecraft attitude determination and control*, edited by J. Wertz, Dordretcht: Kluwer Academic Publishers, 1978.

[4] California Polytechnic State University. *6U Cubesat design Specifications*. Rev. 1, 2018. Available: https://static1.squarespace.com/static/5418c831e4b0fa4ecac1bacd/t/5b75dfcd70a6a dbee5908fd9/1534451664215/6U_CDS_2018-06-07_rev_1.0.pdf Accessed on 20 June 2021.

[5] V. Pisacane. *Fundamentals of Space Systems*. 2nd ed., New York: Oxford University Press, 2005.

[6] J. Wertz, H. F. Meissinger, L. K. Newman and G. N. Smit *Orbit and constellation design and management*. Microcosm Press and Springer, 2001.

[7] C. C. Finlay, N. Olsen, L. Toeffner-Clausen. *The CHAOS-5 Geomagnetic Field Model* [Online] DTU Space, National Space Institute, Technical University of Denmark. Available: http://www.spacecenter.dk/files/magnetic-models/CHAOS-5/. Accessed on 19 June 2021.

[8] S. R. Starin and J. Eterno *Attitude Determination and Control Systems* NASA Goddard Space Flight Center, Greenbelt, MD, USA and Southwest Research Inst. TX, USA, Doc. 20110007876, 2011

[9] J. Trégouët, D. Arzelier, D. Peaucelle, C. Pittet and L. Zaccarian. *Reaction Wheels Desaturation Using Magnetorquers and Static Input Allocation* in IEEE Transactions on Control Systems Technology, vol. 23, no. 2, pp. 525-539, March 2015

[10] BlueCanyon Technologies. *Reaction Wheels data-sheet*. 2020

[11] Hyperion Technologies. *MTQ400 magnetorquer specifications* Available: https://hyperiontechnologies.nl/products/mtq400/ Accessed on 19 June 2021.

[12] NewSpace Systems. *Magnetorquer rod data sheet* Available: https://www.newspacesystems.com/wp-content/uploads/2021/02/NewSpace-Magnetorquer-Rod_2021-10a-1.pdf Accessed on 19 June 2021.

[13] Zynq. *Zynq-7000 Computer data* Available: https://www.xilinx.com/products/silicon-devices/soc/zynq-7000.html Accessed on 30 June 2021.

[14] AAC Clyde Space. *Sirius OBC LEON3FT data sheet* 28 July 2020. Available: https://www.aac-clyde.space/assets/000/000/181/AAC_DataSheet_Sirius_OBC_original.pdf?1614275782 Accessed on 19 June 2021.

[15] NewSpace Systems. *GPS receiver and antenna data sheet* 2020. Available: https://www.newspacesystems.com/wp-content/uploads/2020/10/NewSpace-GPS-Receiver_2020-10a.pdf Accessed on 19 June 2021.

[16] Bidikar, Bharati & Rao, Gottapu & Laveti, Ganesh & Kumar, Mnvs. *Satellite Clock Error and Orbital Solution Error Estimation for Precise Navigation Applications. Positioning.*Vol 05. No 1, 2014, pp. 22-26.

[17] NewSpace Systems. *Magnetometer data sheet* 2020. Available: https://www.newspacesystems.com/wp-content/uploads/2020/10/NewSpace-Magnetometer_2020_10a.pdf Accessed on 19 June 2021.

[18] NewSpace Systems. *Sun Sensors data sheet* 2021. Available: https://www.newspacesystems.com/wp-content/uploads/2021/04/NewSpace-Sun-Sensor_2021-10b.pdf Accessed on 19 June 2021.

[19] T., Wiedermann G., Crombez V., Damilano P. *Pointing budgeting using the ESA Pointing Error Engineering Handbook and Tool: benefits and limitations* in GNC 2014: 9th International ESA Conference on Guidance, Navigation and Control Systems, Porto, Portugal. June 2014

[20] Sensonor. *STIM202 MEMS gyroscope datasheet*. November 2020. Available: https://sensonor.azurewebsites.net/media/ny3dieuq/ts1439-r17-datasheet-stim202.pdf Accessed on 19 June 2020.

[21] Cubespace webpage *Cubesense Star Tracker data sheet* Available: https://www.cubespace.co.za/products/adcs-components/cubestar/ Accessed on 01 July 2021.

[22] F. L. Markley and J. L. Crassidis *Fundamentals of Spacecraft Attitude Determination and Control*. New York: Springer-Verlag. 2014.

[23] H.D., Black: *A passive system for determining the attitude of a satellite.* AIAA J. 2(7),1350–1351. 1964.

[24] M. D. Shuster, S.D. Oh. *Attitude determination from vector observations.* 70–77. 1981.

[25] NASA webpage. *Hubble Telescope Pointing Control* 8 September 2020. Available: https://www.nasa.gov/content/goddard/hubble-space-telescope-pointing-control-system Accessed on 19 June 2021.

[26] Nanosats database. *Figure with the number of satellites launched from 1998 and prediction up to 2025.* Available: https://www.nanosats.eu/ Accessed on 20 June 2021.

[27] Airbus. *New Space. Europe should shape the future of space* Available: https://www.airbus.com/public-affairs/brussels/our-topics/space/new-space.html Accessed 20 June 2021.

[28] Martin Lara Mission Webpage. Available: https://martinlara3.webnode.es/martinlara-mission/ Accessed on 20 June 2021.

[29] Mission Requirements Document of the MartinLara Mission. Available: https://martinlara3.webnode.es/_files/200000038-f175ff1762/MDR_DEFINITIVO.pdf Accessed on 20 June 2021.

[30] T. Terzibaschian, O. Maibaum and C. Raschke. *Definition and implementation of "Attitude Modes" in the DLR small satellites BIRD, TET-1 and BIROS – adoption to developing requirements* in 1st IAA Latin American Symposium on Small Satellites: Session 14. 2018.

[31] A. M. Davis. *Software Requirements: Objects, Functions, and States* Second Edition. 1993.

[32] A. Miró Moncho. *Development and implementation of a DKE space simulator for cubesat missions.*Final Master Thesis. Stellar, University Carlos III of Madrid, 2021.

[33] J. Wertz and W. J. Larson *Space mission analysis and design.* 3rd. edition. Microcosm Press and Kluwer Academic Publisher, 1999.

[34] Gomspace GSW 600 Reaction Wheel data sheet. Available: https://gomspace.com/UserFiles/Subsystems/datasheet/gs-ds-nanotorque-gsw-600-20.pdf Accessed on 27 June 2021.

[35] Madrid Flight on Chip webpage. Available: https://flightonchip.es/ Accessed 30 June 2021.

[36] Gomspace. *NanoMind 3200 On board Computer data sheet.* 17 February 2021. Available: https://gomspace.com/UserFiles/Subsystems/datasheet/gs-ds-nanomind-a3200_1006901-117.pdf Accessed on 19 June 2021.

[37] OCE Technology. Products brochure. Available: http://ocetechnology.com/wp-content/uploads/2017/03/OCEproducts.pdf Accessed on 30 June 2021

[38] Meisei. Magnetometer webpage link. Available: https://www.meisei.co.jp/english/products/space/satellite-components/p1364 Accessed on 30 June 2021

[39] Antrix. Magnetometer webpage link. Available: https://www.antrix.co.in/sites/default/files/Digital%20Miniature%20Magnetometer.pdf Accessed on 30 June 2021

[40] Farnell webpage. Honeywell HMC5843 magnetometer datasheet. Available: http://www.farnell.com/datasheets/926318.pdf Accessed on 30 June 2021

[41] F. Cacciatore. *Attitude dynamics and GNC* Lecture notes, UC3M *Máster Universitario en Ingeniería Espacial* 2020-2021.

[42] *KU Leuven star tracker datasheet.* http://www.cubesatpointing.com/DownloadFiles/Datasheets/KULSTDatasheet.pdf Accessed on 01 July 2021.

[43] Farnell Webpage *MPU-3300 gyroscope datasheet.* http://www.farnell.com/datasheets/2645525.pdf Accessed on 01 July 2021.

[44] M. J. Sidi. *Spacecraft dynamics and control.* Cambridge: Cambridge University Press, 1997.